

# 1 Evaluating an Earth system model from a water manager user 2 perspective

3

4 Mari R. Tye<sup>1,2</sup>, Ming Ge<sup>1</sup>, Jadwiga H. Richter<sup>1</sup>, Ethan D. Gutmann<sup>1</sup>, Allyson Rugg<sup>1</sup>, Cindy L.  
5 Bruyère<sup>3</sup>, Sue Ellen Haupt<sup>1</sup>, Flavio Lehner<sup>4,1,5</sup>, Rachel McCrary<sup>1</sup>, Andrew J. Newman<sup>1</sup>, Andy  
6 Wood<sup>1,6</sup>

7 1 National Center for Atmospheric Research, Boulder, CO

8 2 Whiting School of Engineering, Johns Hopkins, Baltimore, MD, USA

9 3 Cooperative Programs for the Advancement of Earth System Science (CPAESS), UCAR, Boulder, CO

10 4 Department of Earth and Atmospheric Sciences, Cornell University, Ithaca, NY, USA

11 5 Polar Bears International, Bozeman, MT, USA

12 6 Department of Civil and Environmental Engineering, Colorado School of Mines, Golden, CO, USA

13 Correspondence to: Mari R. Tye (maritye@ucar.edu)

## 14 Abstract

15 The large spatial scale of global Earth system models (ESM) is often cited as an obstacle to using the output by  
16 water resource managers in localized decisions. Recent advances in computing have improved the fidelity of  
17 hydrological responses in ESMs through increased connectivity between model components. However, the  
18 models are seldom evaluated for their ability to reproduce metrics that are important for practitioners, or present  
19 the results in a manner that resonates with the users. We draw on the combined experience of the author team  
20 and stakeholder workshop participants to identify salient water resource metrics and evaluate whether they are  
21 credibly reproduced over the conterminous U.S. by the Community Earth System Model v2 Large Ensemble  
22 (CESM2). We find that while the exact values may not match observations, aspects such as interannual  
23 variability can be reproduced by CESM2 for the mean wet day precipitation and length of dry spells. CESM2  
24 also captures the proportion of annual total precipitation that derives from the heaviest rain days in watersheds  
25 that are not snow-dominated. Aggregating the 7-day mean daily runoff to HUC2the watersheds scale also shows  
26 rain-dominated regions capture the timing and interannual variability in annual maximum and minimum flows.  
27 We conclude there is potential for far greater use of large ensemble ESMs, such as CESM2, in long-range water  
28 resource decisions to supplement high resolution regional projections.

## 29 1 Introduction

30 Water availability and water quality for human consumption, ecosystems, and agriculture are fundamental  
31 requirements, making pertinent assessments of future change crucial for adaptation planning (IPCC, 2022).  
32 Climate related changes in the hydrologic cycle will affect substantial portions of the world population, most  
33 directly through changes in water availability at or near the surface (Mankin et al., 2020; Sedláček and Knutti,  
34 2014). The information required by water resource managers for decision making is not readily available in a

35 relevant format, or at sufficient spatial or temporal resolutions from global Earth system models (ESM; e.g.,  
36 Ekström et al., 2018). We explore how the Community Earth System Model (CESM) represents the climatology  
37 of water availability, focussing on metrics that are familiar to decision makers in planning investment-scale  
38 decisions.

39 The inability of ESMs to explicitly resolve sub-grid scale (~100 km) processes is often cited as the limitation  
40 preventing direct model use in decision making. Literature from large organizations making infrastructure  
41 decisions (e.g., Brekke, 2011; Brekke et al., 2009; Reclamation, 2016, 2014) emphasize downscaling climate  
42 model data closer to the scale of the watersheds they manage. These additional modeling steps add complexity  
43 and may increase statistical errors (Clark et al., 2015; Ekström et al., 2018). Extracting useful and robust  
44 information directly from ESMs would reduce such errors if metrics most important to decision makers, such as  
45 the timing of peak flow, were known to be robustly represented.

46

47 There are many comprehensive examples of metrics used to evaluate climate and hydrological models (e.g.,  
48 Ekström et al., 2018; Mizukami et al., 2019; Wagener et al., 2022), and communicate the impacts of climate  
49 change (e.g., Reed et al., 2022), or to identify decision-relevant metrics (e.g., Bremer et al., 2020; Mach et al.,  
50 2020; Underwood et al., 2018; Vano et al., 2014). However, very few have examined whether user defined  
51 metrics can be reliably reproduced by ESMs (Mankin et al., 2020), and if further model development and scale  
52 reduction is warranted instead of improved communication (Pacchetti et al., 2021). Better communication may  
53 also reduce the temptation of some users to calculate “standard hydroclimate metrics” that are not supported by  
54 the climate model data (Ekström et al., 2018).

55

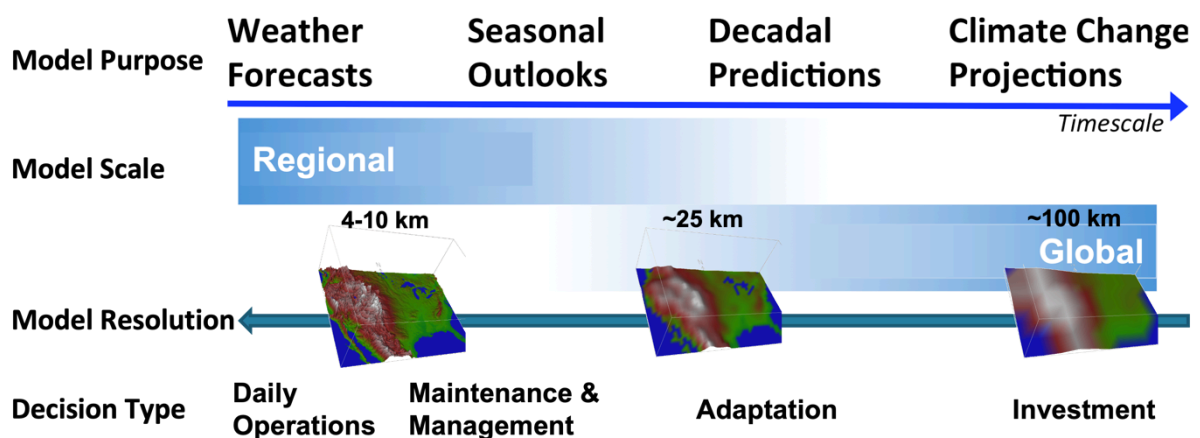
56 In contrast, climate model output can be rejected unnecessarily when simulated annual minima from freely  
57 running simulations do not “match” the sequence of observed low flows (Ekström et al., 2018; Moise et al.,  
58 2015). Similarly, the benefits of a range of projected outcomes from different climate models are not widely  
59 appreciated beyond the climate model community (Tebaldi and Knutti, 2007). Large ensembles from a single  
60 climate model initialized with a range of atmospheric and ocean conditions, such as the CESM2 Large  
61 Ensemble (LENS2; Rodgers et al., 2021), help to bound the uncertainty that derives from a naturally chaotic  
62 system. Averaged over the full ensemble, they give a better estimate of the model’s response to internal and  
63 external forcing (Deser et al., 2012) and enable assessments of the rarity of projected extremes. The additional  
64 analysis to identify structural (i.e. model formulation) and internal variability within regional climate models  
65 means that there are fewer large ensembles at a high resolution (Deser et al., 2020).

66

67 Since different decision makers have different priorities and time-scales of interest, Shepherd et al. (2018)  
68 recommended the development of climate storylines to communicate with those using climate data to make  
69 decisions. Informed by prior surveys of water managers (e.g., Brekke, 2011; Brekke et al., 2009; Cantor et al.,  
70 2018; Raff et al., 2013; Wood et al., 2021), Fig. 1 aims to map the different types of water decisions (e.g., Raff  
71 et al., 2013 Fig. 3) to the different scales of model resolution (Meehl et al., 2009 Fig. 2). Water managers make  
72 daily operational decisions (e.g., to control instantaneous river flow) with the aid of fine-scale weather and flood  
73 models (<4 km) that reliably represent convective and local weather scale processes even though their

74 predictability is relatively short lived (Yuan et al., 2019; far left side of Fig. 1). Larger watershed operations  
 75 (such as reservoir management or groundwater recharge; e.g., Regional Water Authority, 2019) depend on  
 76 seasonal outlooks (middle left of Fig. 1). Smaller adaptation and mitigation projects take place at the typical  
 77 policy or decadal prediction scale (i.e., 4-10 years; middle right of Fig. 1). Finally, major public investments and  
 78 inter-basin agreements occur at the same time scales as climate projections (30-100 years; far right of Fig. 1)  
 79 where persistent and relatively predictable synoptic and planetary scale processes are well represented in lower  
 80 resolution (~100 km) climate models (Phillips et al., 2020). While forecasts (seasonal or decadal) are  
 81 re-initialized from specific atmosphere, ocean or land states at regular time intervals, climate projections are run  
 82 freely from a variety of atmospheric and oceanic conditions that take several decades to converge to a mean  
 83 climatology. In considering the utility and useability of information directly from ESMs we focus on decisions  
 84 made over decadal to climate scales at larger spatial scales.

85



86

87 **Figure 1: Mapping the temporal and spatial scales of models to the timeframes for water management decisions.**

88 Given that ESMs have advanced immeasurably in the recent decade, it is time to re-evaluate whether their direct  
 89 output can support decision makers. Such an evaluation needs to focus on how well the models can reproduce  
 90 metrics used by decision makers, and whether the results are credible (Briley et al., 2020; Jagannathan et al.,  
 91 2021). Here we evaluate the credibility of one ESM in generating metrics known to be salient for water  
 92 management decisions; specifically, decisions for water management infrastructure project investments.

93

94 The motivation for this paper is to identify:

- 95 • a set of water availability metrics that resonates with decision makers and supports their
- 96 investment-scale decisions;
- 97 • how well CESM2 represents the climatology and recent observed behaviors of those metrics; and
- 98 • how such metrics are projected to change.

99

100 This paper builds off a decade of collaboration between scientists at the National Center for Atmospheric  
 101 Research (NCAR) and US water agencies that lead to a virtual workshop (Tye, 2023), and presents a test case  
 102 for improved communication with water resources decision makers. The focus is on the Conterminous United  
 103 States (CONUS) to match the interest of workshop participants.

## 104 2 Climate Information Needs from Prior Research

105 Information needs vary greatly, from 5-minute rainfall totals at a point (ASCE, 2006), to basin-wide measures of  
106 annual minimum and maximum total runoff. Water management decision metrics can be grouped into similar  
107 types such as timing, frequency, magnitude, extreme values, variability, and duration of events (Ekström et al.,  
108 2018). While some aspects of timing, magnitude, or variability can be reliably reproduced by ESMs (e.g., Deser  
109 et al., 2020; Tebaldi and Knutti, 2007), others such as short duration extremes are less reliable.

110

111 Methods of evaluation and data use also differ. For instance, Clifford et al. (2020) reported that predicting  
112 general changes in the frequency of extreme precipitation events is more useful for future planning than the  
113 precise prediction of mean values evaluated by model developers. Lehner et al. (2019) emphasized that models  
114 need to be evaluated for their ability to reproduce sensitivities (e.g., streamflow changes in response to  
115 temperature and precipitation changes) in addition to mean states. However, metrics that are meaningful for  
116 evaluating a model's capabilities (e.g., the ratio of precipitation to runoff) are less valuable for management  
117 decisions (Lehner et al., 2019; McMillan, 2021; Mizukami et al., 2019). When reporting results, **water**  
118 **managers/users** are more familiar with the 'water year', rather than the calendar year, to capture the full annual  
119 hydrological cycle (Ekström et al., 2018). While the use of water years is a nuance that does not add substantial  
120 value to climate model assessments, communication with decision makers is improved by presenting data in a  
121 familiar format (Briley et al., 2020).

122

123 There is a need for information at the local scale that is unlikely to be met directly by raw outputs from the  
124 current generation of ESM. But better communication of the variability in future daily precipitation and  
125 associated runoff can add value to the detailed models by bringing in the added statistical context and  
126 perspective of the large ensembles. Thus, we believe that ESMs can produce useful information about  
127 hydro-meteorological extremes when presented at different spatial or temporal scales, and offer the benefits of  
128 large climate model ensembles to constrain future impact uncertainty.

129

130 Appendix A summarizes potential hydrological metrics used in water management decisions (Jagannathan et al.,  
131 2021) or statistical assessments of extremes (Zhang et al., 2011), and model evaluations (Phillips et al., 2020).  
132 Metrics in bold are presented in this paper. We only considered a simplistic measure of meteorological drought  
133 (absence of rain) in the current work, as drought is sensitive to the definition (Bachmair et al., 2016) and local  
134 conditions (Mukherjee et al., 2018), and so not suited to a generalized assessment. Similarly, snow measures are  
135 not included in this assessment ~~—~~in part due to limited availability of high-quality, long-duration,  
136 quality-controlled, observational data (McCrary et al., 2017); and **partly due to** the biases in snow distribution  
137 arising from the smoothed topography in GCMs (McCrary et al., 2022).

138 **3 Data and Methods**

139 **3.1 Climate Model Data**

140 CESM2 (Danabasoglu et al., 2020) is a fully coupled global model that simulates the Earth’s climate system  
141 through interactive models for atmosphere, ocean, land, sea-ice, river runoff, and land-ice. Variables considered  
142 in this project are taken from the Community Atmosphere Model version 6 (CAM6) and the Community Land  
143 Model version 5.0 (CLM5; Lawrence et al., 2019) and are part of the default model outputs. A schematic of the  
144 model components is included in Appendix B. This project uses daily values scaled up to annual (e.g., annual  
145 maximum daily precipitation) on a ~1 degree resolution grid. Data were extracted over the CONUS from 10  
146 ensemble members of LENS2 (Rodgers et al., 2021) for model validation in the current era (1981-2010), ~~and a  
147 future time period (2041–2070) under the Shared Socioeconomic Pathway emissions scenario SSP2-4.5 (Riahi et  
148 al., 2017). This emissions scenario represents a world where “social, economic, and technological trends do not  
149 shift markedly from historical patterns” (O’Neill et al., 2017).~~

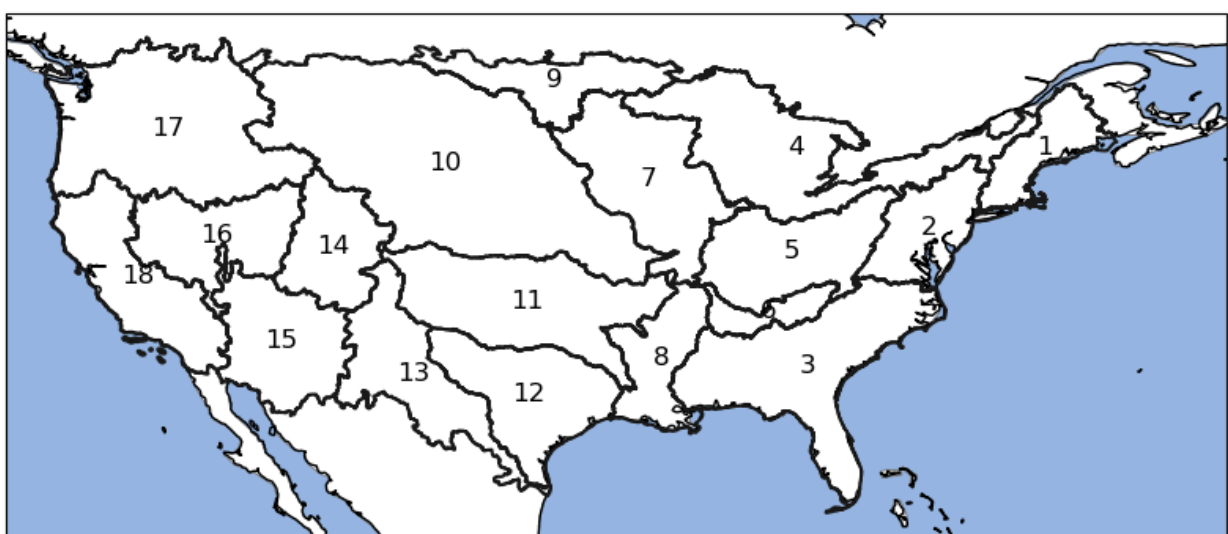
150 **3.2 Observations**

151 Gridded daily observations of precipitation at 1/16° horizontal resolution (~6 km) were obtained from the  
152 Livneh et al. (2013) dataset covering CONUS and southern Canada for the control period (1981-2010), hereafter  
153 referred to as “Livneh”. While the time adjustment in the Livneh dataset results in an underestimation of the  
154 most extreme daily precipitation totals and resultant runoff and flood potential (Pierce et al. 2021), we are also  
155 interested in precipitation and runoff minima. As a result we did not employ the updated gridded observations  
156 (Pierce et al. 2021).

157

158 Livneh daily temperature maxima and minima, and precipitation were used to force the Variable Infiltration  
159 Capacity Model (VIC; Liang et al., 1994) version 4.1.2 to obtain runoff estimates for years 1980-2005 as  
160 evaluated in Livneh et al. (2013). Hereafter referred to as “Livneh-VIC”.

161



162

163 Figure 2: HUC 2 regions used in data validation and analysis. Regions defined by USGS (2013): Region 01 New  
164 England (NE); Region 02 Mid-Atlantic (MA); Region 03 South Atlantic-Gulf (SA); Region 04 Great Lakes (GL);  
165 Region 05 Ohio (OH); Region 06 Tennessee (TN); Region 07 Upper Mississippi (UM); Region 08 Lower Mississippi  
166 (LM); Region 09 Souris-Red-Rainy (RR); Region 10 Missouri (MR); Region 11 Arkansas-White-Red (ARK); Region  
167 12 Texas-Gulf (GUL); Region 13 Rio Grande (RIO); Region 14 Upper Colorado (UC); Region 15 Lower Colorado  
168 (LCO); Region 16 Great Basin (GB); Region 17 Pacific Northwest (PN);  
169 Region 18 California (CA)

### 170 3.3 Methods

171 All analyses were carried out using the North American water year (1 October to 30 September) to facilitate  
172 later communication.

#### 173 3.3.1 Remapping

174 For ease of comparison, model output were re-gridded using a conservative second-order remapping (Jones,  
175 1999) to place both datasets on the same scale grid and assess anomalies. Data were also calculated as areal  
176 averages or totals over the 2-digit Hydrological Unit Code (HUC2) regions (Seaber et al., 1987). HUC2 basins  
177 represent 18 watersheds, covering areas ranging from 41,000 mi<sup>2</sup> (~105,000 km<sup>2</sup>; Tennessee) to 520,960mi<sup>2</sup> to  
178 (1,350,000 km<sup>2</sup>; Missouri), shown in Fig. 2. While the scale of HUC2 regions may be large for some local  
179 decision-makers, it is also a more appropriate and conservative scale to compare to ESMs as demonstrated by  
180 Lehner et al. (2019).

#### 181 3.3.2 Percentile-based thresholds

182 The threshold for very heavy rain days (Q95) was calculated at each individual grid cell using only days with  $\geq$   
183 1 mm rain (“wet days”). Thresholds were ~~derived empirically~~ ~~calculated~~ for each model ensemble member, with  
184 the ensemble mean threshold (Q95) used to ~~identify the estimate the future number of~~ days per year (exceeding  
185 the threshold (N95) and total annual rainfall from those days (P95). ~~Q95 was not re-evaluated for the future~~  
186 ~~climatological period.~~  
187

188 Runoff was aggregated over each HUC2 watershed and multiplied by the respective area ~~of~~ to generate total  
189 volume per day. Volume per day was then converted to measurements more familiar to users, such as acre feet  
190 per day or cubic meters per second. Daily time series of total volumetric runoff had a 7-day running mean  
191 smoother applied, then annual maximum, minimum and mean values were extracted. The highest and lowest  
192 7-day average runoff expected once per decade (7Q90, 7Q10) were estimated ~~empirically~~ from ~~the 25 ranked~~  
193 ~~values of twenty five years of~~ annual maxima and minima ~~per watershed~~.

## 194 4 Model Evaluation

195 The metrics used to evaluate CESM2’s ability to reproduce large scale features and physical behaviors (e.g.,  
196 Danabasoglu and Lamarque, 2021 and the associated Special Issue) are not necessarily those employed by  
197 decision makers. ESMs are designed to represent large-scale atmospheric processes and fluxes not specific local  
198 responses (Gettelman and Rood, 2016), but this design assumption may not be sufficiently well communicated  
199 to decision makers. The purpose of our evaluation is to establish whether CESM2 output is also fit for local

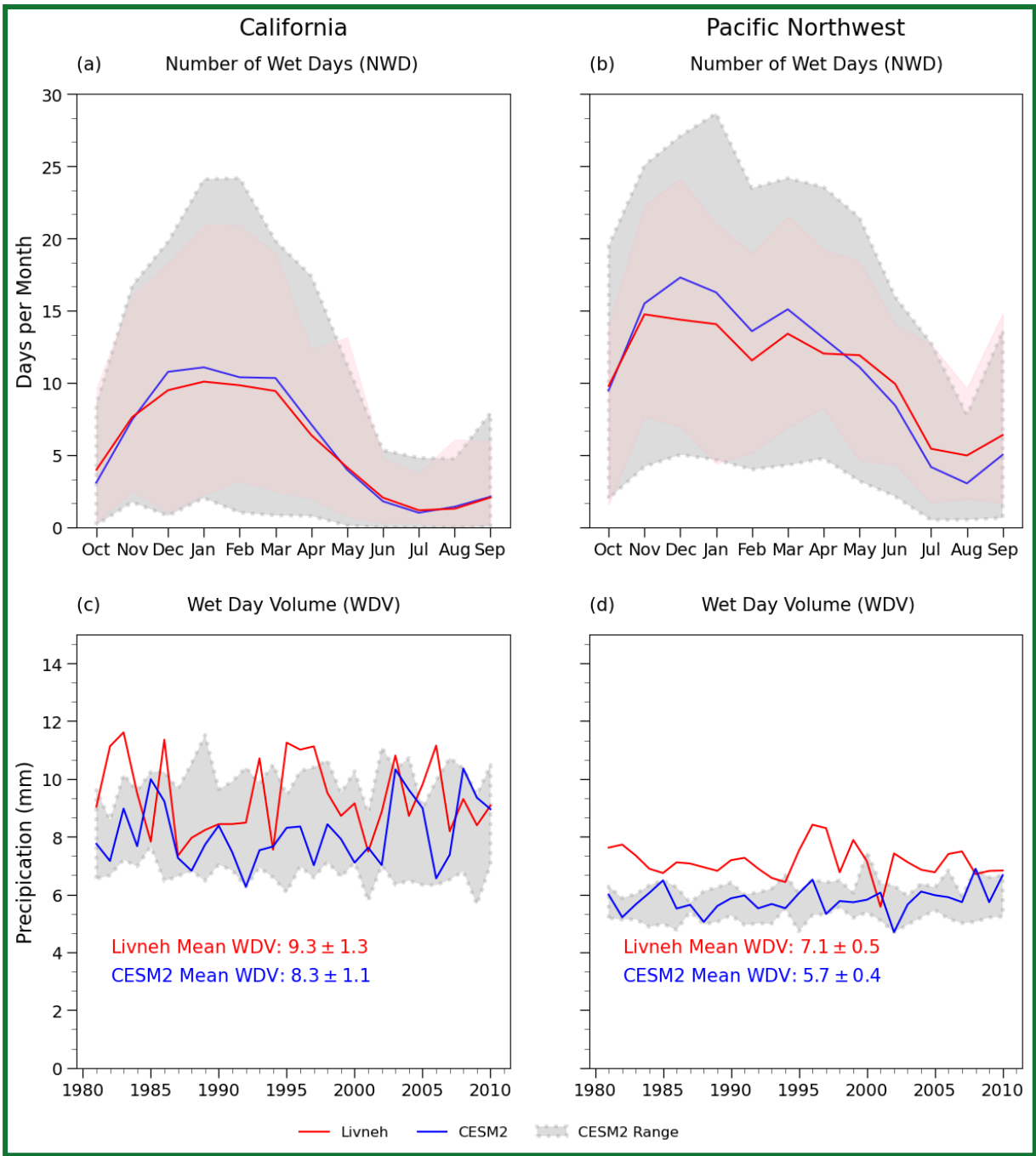
200 decision purposes, or if the breadth of information from ESM ensembles remains unsuitable for immediate use  
201 in targeted water management decisions.

#### 202 4.1 Rainfall metrics

203 While broad spatial patterns of seasonal mean daily rainfall are reproduced well (Danabasoglu et al., 2020; Feng  
204 et al., 2020; Simpson et al., 2022), CESM2 fails to capture details over high topography, and overestimates  
205 summer precipitation where convective extremes dominate summer rainfall (Appendix B). The seasonal mean  
206 precipitation also fails to capture some important watershed-level processes, such as the seasonal variability in  
207 the number of days with precipitation and the associated intensity.

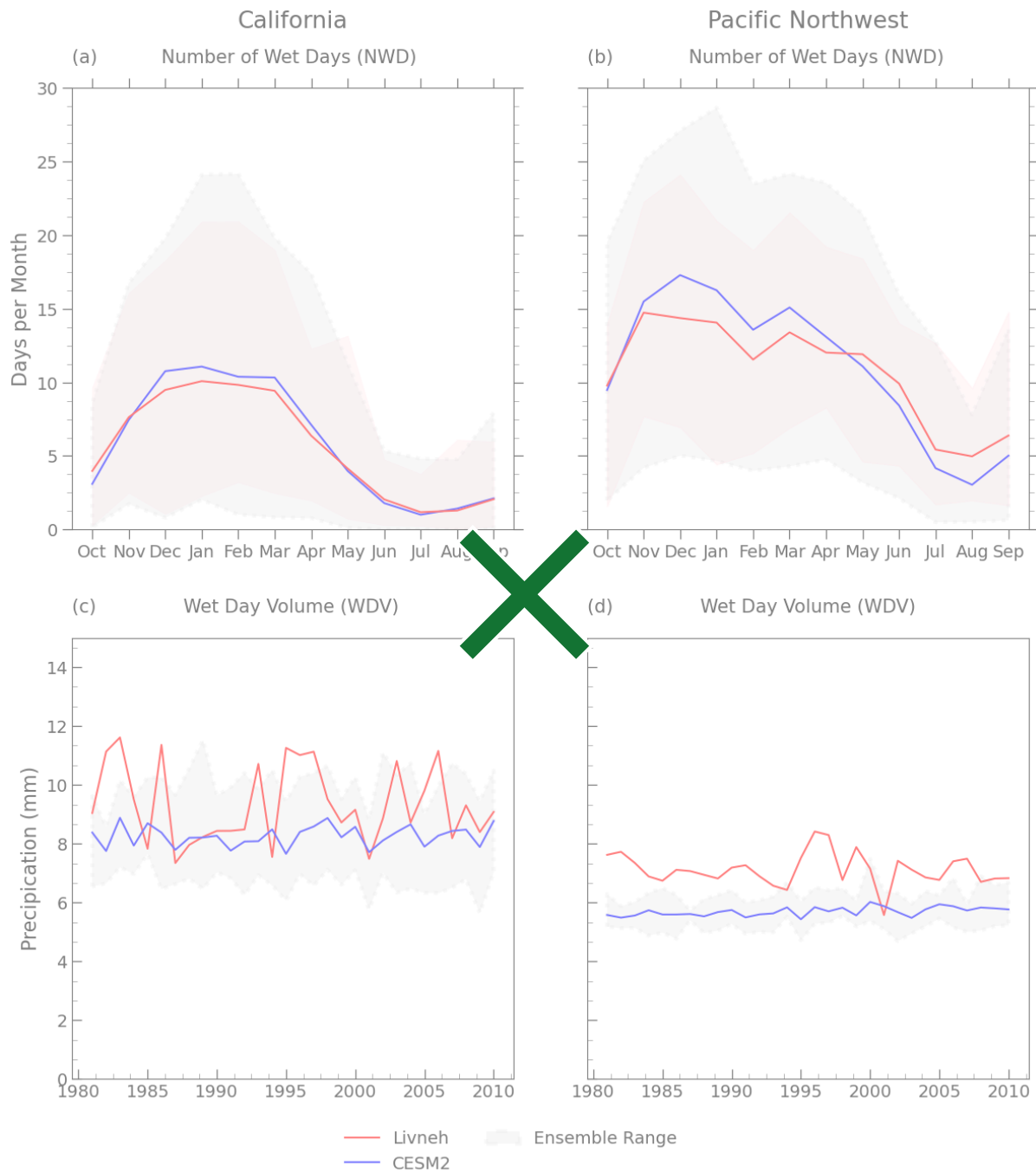
208

209 Estimates of mean annual rainfall on wet days, or wet day volume, are in broad agreement between Livneh and  
210 CESM2 output. Figure 3 shows an example of the mean number of wet days per month (NWD), and mean wet  
211 day volume (WDV) averaged over the Mid Atlantic and Pacific Northwest. While CESM2 represents the NWD  
212 annual cycle very well in regions such as California (Fig. 3a, 3c) and the Pacific Northwest (Fig. 3b, 3d), it does  
213 not capture NWD in many central and snow dominated regions. This is likely due to the smoother topography of  
214 CESM2 missing the influence of orographic uplift, and large spatial scale missing sub-grid scale convective  
215 systems (e.g., over the Central Plains).



216





217

218 Figure 3: Average number of wet days per month (a, b) and interannual variability in mean annual precipitation on  
 219 wet days for Livneh climatological mean (red) with interannual spread (pink) and CESM2 mean (blue) with  
 220 interannual and ensemble spread (gray); and (c,d) between 1981-2010 for observations derived from Livneh (red)  
 221 and CESM2 ensemble mean (blue) and spread (gray) in (a,c) Region 18 California (CA);  
 222 and (b,d) Region 17 Pacific Northwest (PN).

223 The annual variability in WDV, both year-to-year variations as well as the overall range of minima and maxima,  
 224 is well captured by each of the model members for the different HUC2 regions, even if the absolute values do  
 225 not match (Fig. 3 c,d). As expected, the specifics of which years have high or low values of WDV are not the  
 226 same for each ensemble member (i.e. demonstrating internal variability). As a result, the ensemble mean value  
 227 of WDV (blue) does not reflect the same year-to-year variability as the observations. Decision makers expressed

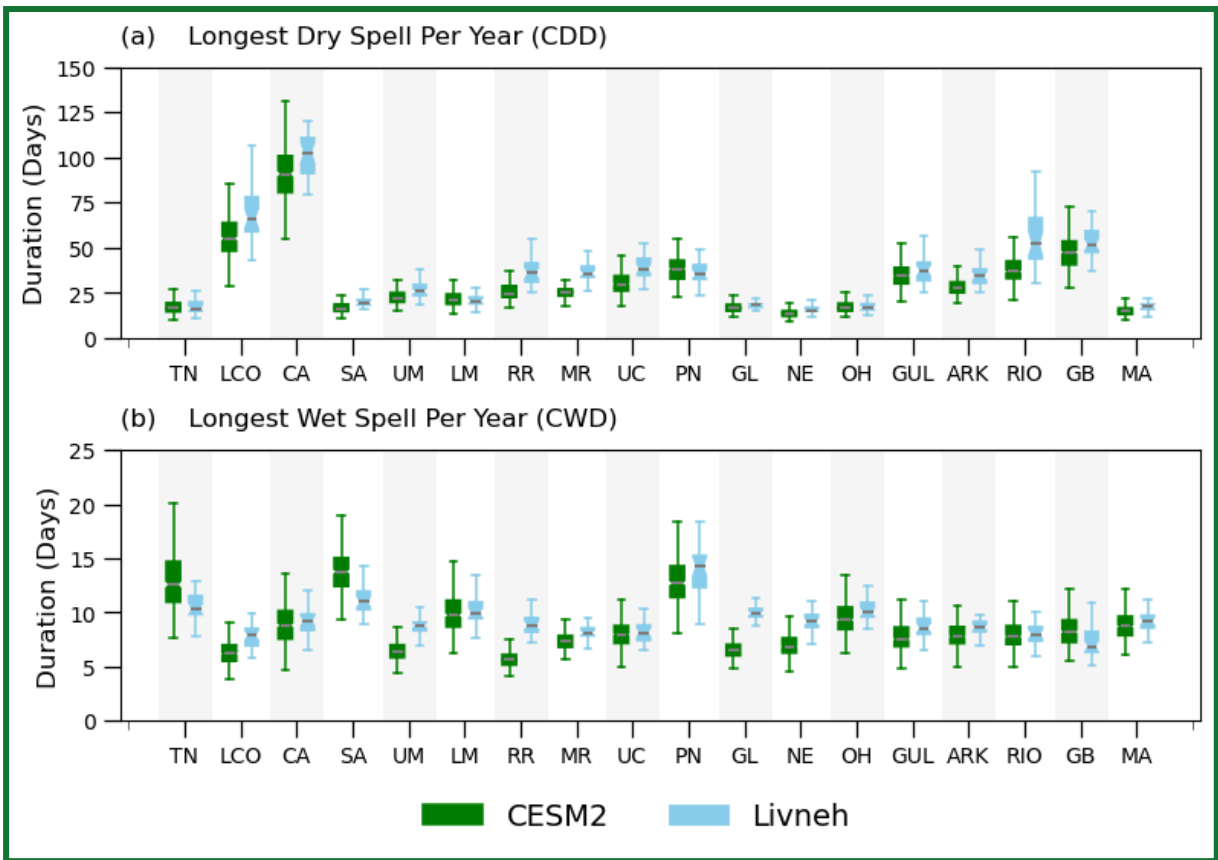
228 that the interannual variability demonstrated by each model member is more valuable to demonstrate the  
229 credibility of the data than the ensemble mean (Tye, 2023). We recommend that the full range of values of each  
230 metric (i.e. after computation for each ensemble member individually) are communicated in addition to the  
231 climatological means to help bound uncertainty around decisions (Wilby et al., 2021).

232

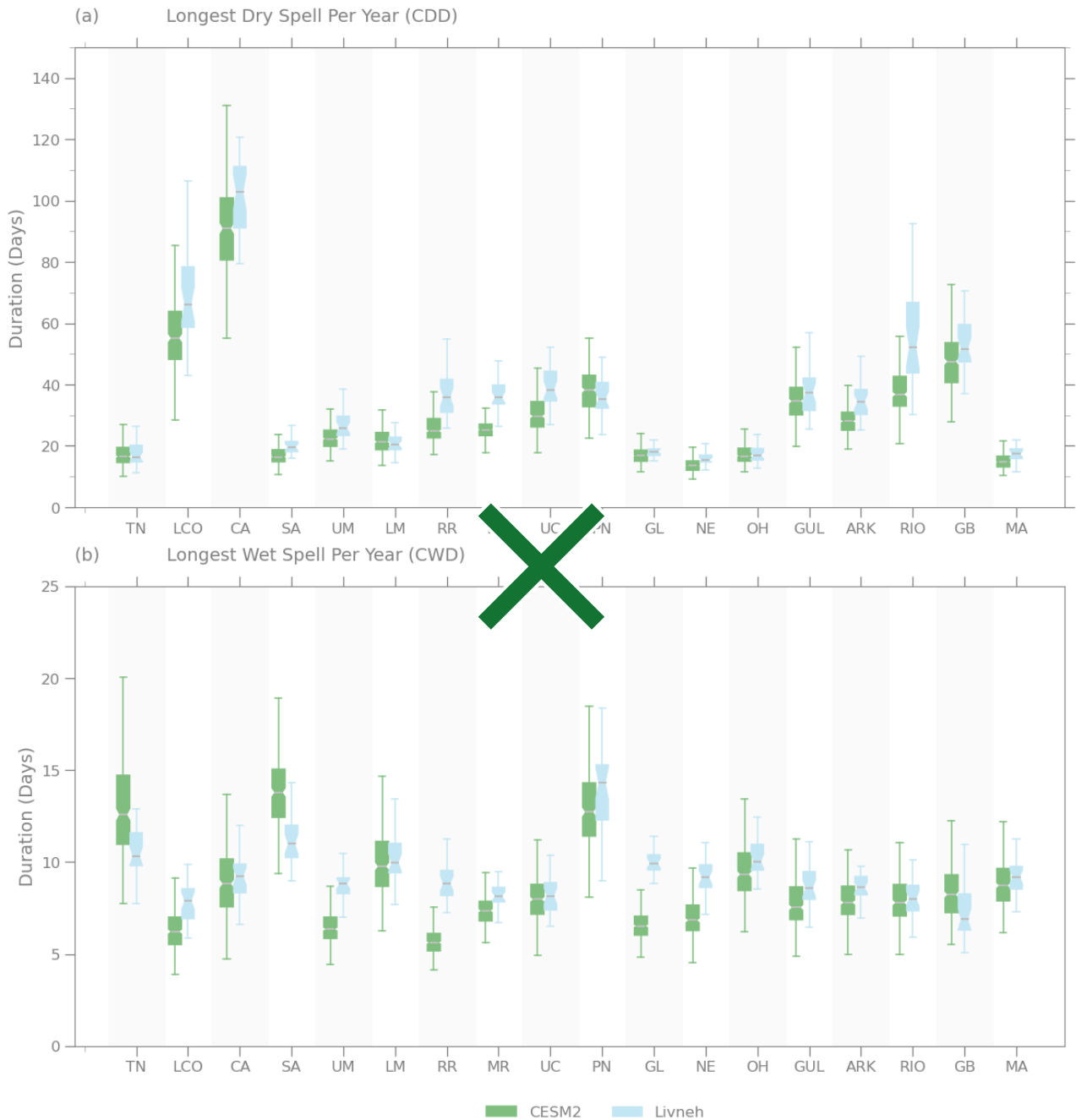
233 The magnitude of interannual variability in WDV (i.e., the absolute differences between the maximum and  
234 minimum values in each member time series) is typically within 10% of observations in all regions as illustrated  
235 for two regions in Fig. 3. Exceptions are the Lower Colorado, South Atlantic-Gulf and Upper Mississippi where  
236 the simulated distributions are too narrow. ~~Many different sources of error may contribute to this discrepancy,~~  
237 ~~such as the inability to resolve convective precipitation (Chen et al., 2021) in addition to~~ ~~While not as~~  
238 ~~mountainous as, say, Upper Colorado these regions have a wide range of elevation changes not captured by the~~  
239 ~~coarse model resolution, or the “drizzle effect” that is common in GCMs (Chen et al., 1996; Dai, 2006) that may~~  
240 ~~contribute to the model-observation differences.~~

241

242 CESM2 captures the longest spells of consecutive dry days per year (CDD; Fig. 4a) and consecutive wet days  
243 per year (CWD; Fig. 4b), and their variability. Many regions capture both the interannual variability and the  
244 climatological mean duration of CWD, particularly those regions that are subject to large-scale synoptic systems  
245 (e.g., Pacific Northwest, Mid Atlantic-Gulf, California). Several regions either overestimate (South  
246 Atlantic-Gulf) or underestimate (Great Lakes, Souris-Red-Rainy) the absolute durations of the longest wet  
247 spells, but do reflect the magnitude of interannual variability. The exception is Tennessee, where both  
248 interannual variability and mean CWD are overestimated. At the grid scale, broad spatial patterns of CWD are  
249 correct but the finer atmospheric processes arising from topographic features are incorrect, as expected from the  
250 coarse model resolution. A similar pattern is present in CDD, except that some drier regions with CDD >30 days  
251 do not capture the full range of interannual variability (Souris-Red Rainy, Missouri, Rio Grande). ~~As This is~~  
252 ~~likely because all GCMs have a tendency to produce drizzle, (Chen et al., 1996; Dai, 2006; Vano et al., 2014);~~  
253 adjusting for a higher wet day threshold (e.g., 2 mm) might improve dry spell representation in those regions. It  
254 is also important to communicate such model sensitivities to users more effectively.



255



256

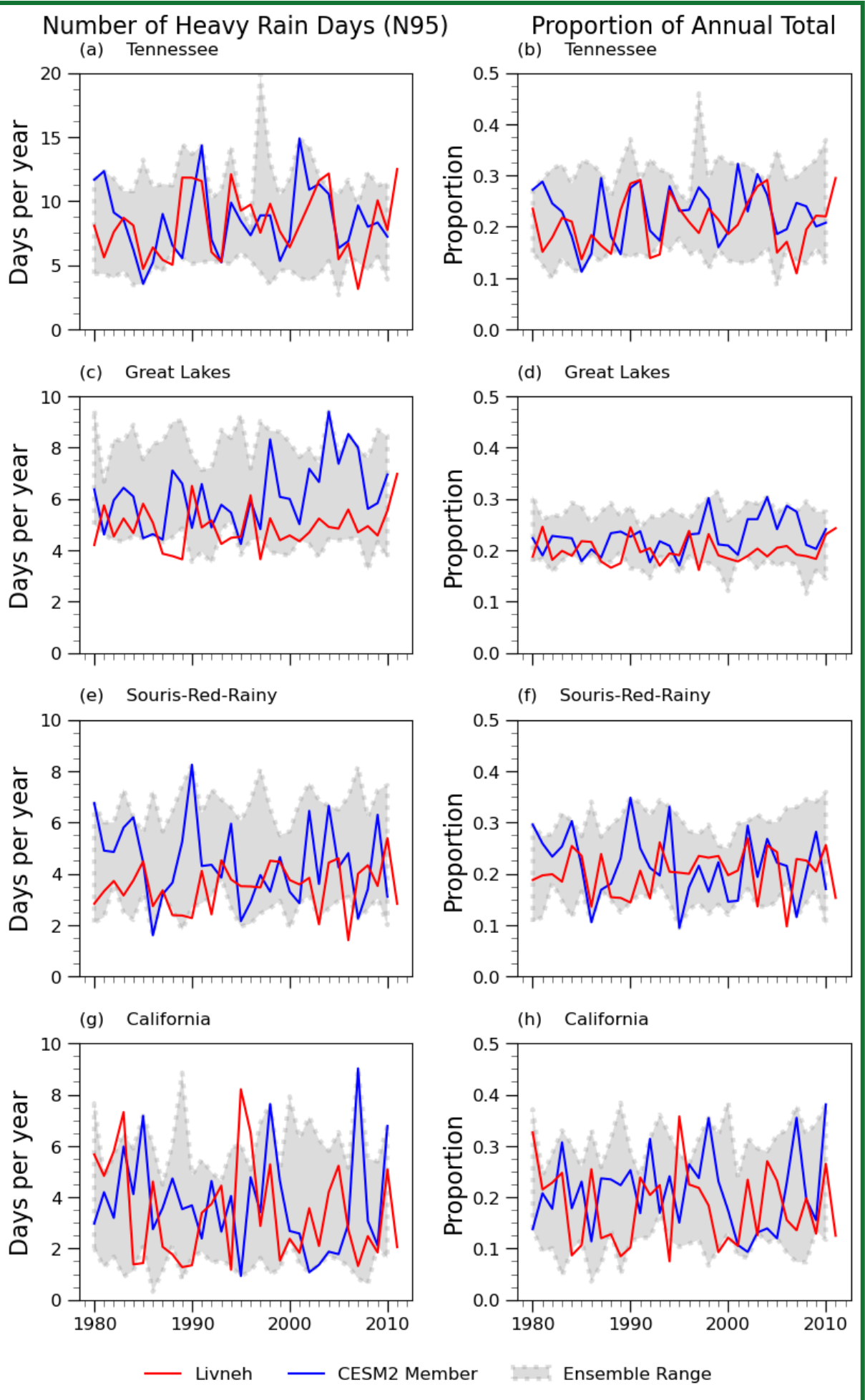
257 **Figure 4: a) Longest duration per year of consecutive days <1 mm rain (longest dry spell) for Livneh over all years**  
 258 **(green) and CESM2 ensemble range over all years (blue) for all HUC2 regions; and b) Longest duration per year of**  
 259 **consecutive days with  $\geq 1$  mm rain (longest wet spell). Regional Acronyms defined in Fig. 2.**

260 The thresholds for heavy and very heavy rain days (P95, P99) are defined individually for Livneh and CESM2  
 261 both to understand whether the intensity of more extreme rainfall is captured, and to evaluate model behavior. A  
 262 comparison of the thresholds reflects the considerable improvements in modeling capabilities in recent years  
 263 (Gettelman et al., 2022). For instance, earlier versions of CESM underestimated extreme precipitation intensity  
 264 by 10-30 mm/day east of the Rockies, and overestimated intensity by 5-10 mm/day to the west (Gervais et al.,  
 265 2014). We found CESM2 still underestimates the most extreme rainfall, but that errors have approximately  
 266 halved. As these differences are still inadequate for many engineering and major infrastructure decisions

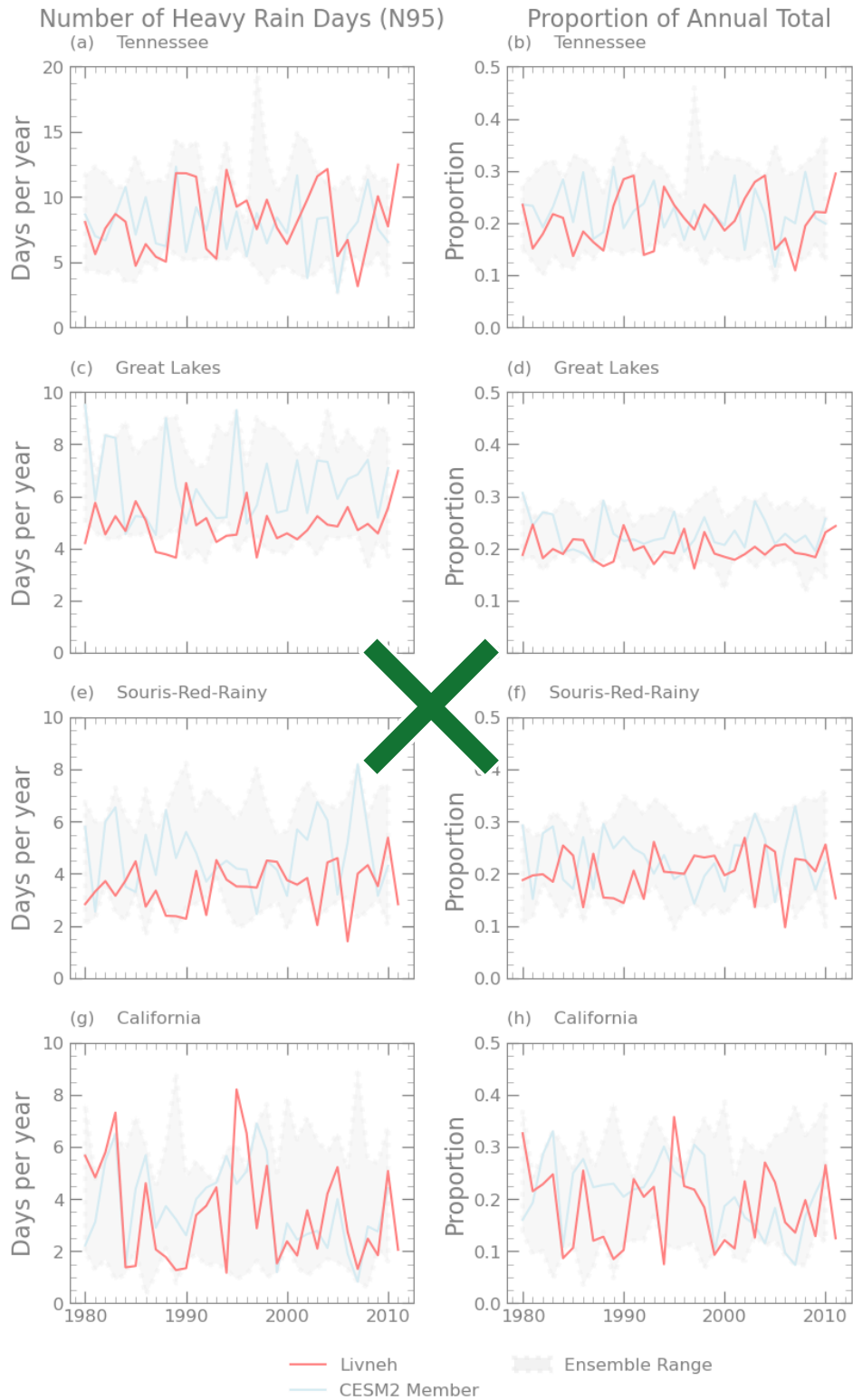
267 (Wright et al., 2019), we focus on CESM2's ability to capture the ~~relative contributions~~ ~~frequency~~ of P95 and  
268 P99 ~~per year, and their relative contributions~~ to the annual total ~~and the interannual variability in their~~  
269 ~~frequency~~. A result with considerable useability is the proportion of annual total precipitation derived from the  
270 heaviest rain days, or "Proportional Contribution of Extreme Days" (P95Tot). This proportion and its  
271 interannual variability is well represented by CESM2 at the HUC2 scale and has shown to be skillful in other  
272 models (Tebaldi et al., 2021).

273

274 The interannual variability in the frequency (N95) and intensity of extreme rainfall, as represented by P95Tot,  
275 are illustrated in Fig. 5 and 6. In several HUC2 regions the simulations report more frequent events, and  
276 proportionally higher totals (e.g., Great Lakes, Rio-Grande, Missouri, Upper Colorado and Lower Colorado).  
277 Overall, there is good agreement between Livneh and CESM2, identifying an opportunity to inform local  
278 decisions from large scale ESMs.

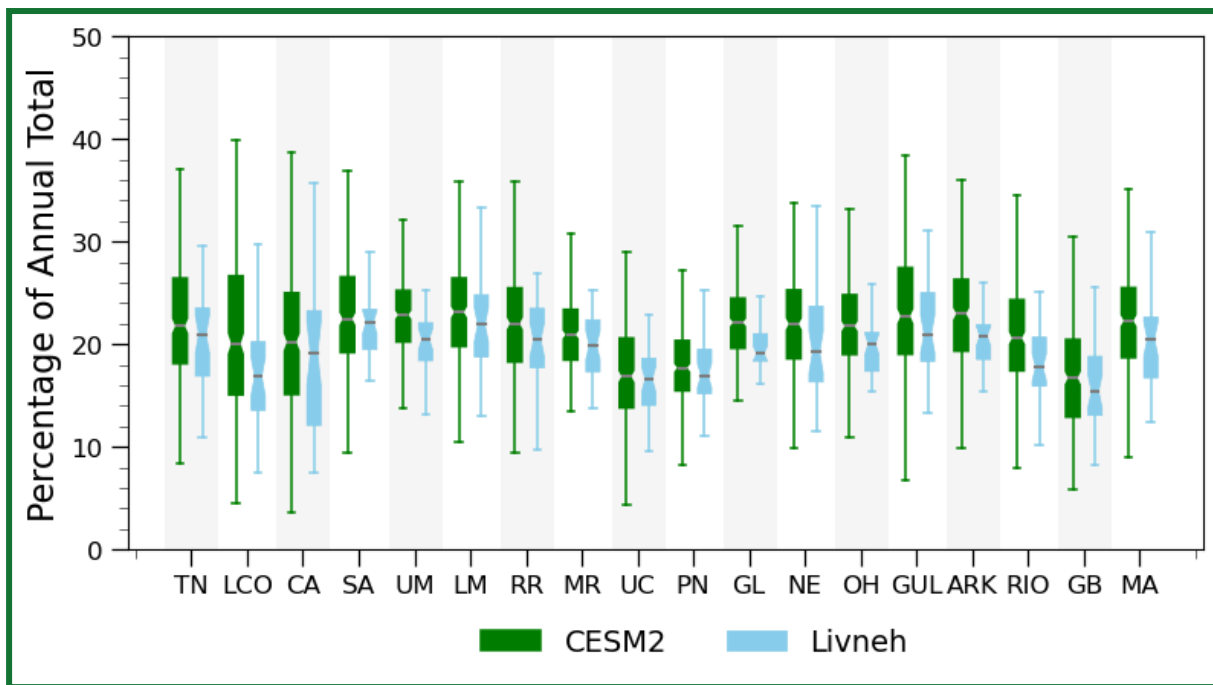


— Livneh    — CESM2 Member    Ensemble Range



280

281 Figure 5: a, c, e, g) Number of very heavy rain days per year; and b, d, f, h) total rain from very heavy rain days as a  
 282 proportion of the annual total for a, b) Tennessee (TN); c,d) Great Lakes (GL); e,f) Souris-Red-Rainy (RR); and g,h)  
 283 California (CA) HUC2 regions. Observations in red; CESM2 ensemble spread in gray, single ensemble member in  
 284 blue.



285  
 286 Figure 6: Box plots of the interannual range of contributions to annual total rainfall from very heavy days (P95Tot)  
 287 shown as percentages for: Observations (light blue), and ensemble range for CESM2 (green) for all HUC2 regions.  
 288 Boxes are bound by the interquartile range, black lines indicate the median, notches indicate the degree of spread  
 289 from the median and bars extend to the full data range.

#### 290 4.2 Runoff metrics

291 Runoff estimates are taken from the individual components of surface and subsurface runoff generated within  
 292 CLM5 (Lawrence et al., 2019) and compared to the Livneh forced VIC runoff (“Livneh-VIC”).

293

294 Assessing the skill of runoff in large-scale models is complicated by many factors, including the mismatch of  
 295 scales between in-channel flow ( $\sim 1\text{-}10^2$  m) and the grid scale ( $\sim 10^5$  m). Thus, metrics of climate model runoff  
 296 should be selected carefully and the runoff should be aggregated or combined with other metrics, rather than  
 297 used directly (Lehner et al., 2019). Appendix C demonstrates the discrepancies between the grid-scale  
 298 representation of runoff from Livneh-VIC and CESM2. The large discrepancies arise from different processes  
 299 that are not captured adequately, such as groundwater, topography, and associated snow ablation and melt, in  
 300 addition to meteorological biases.

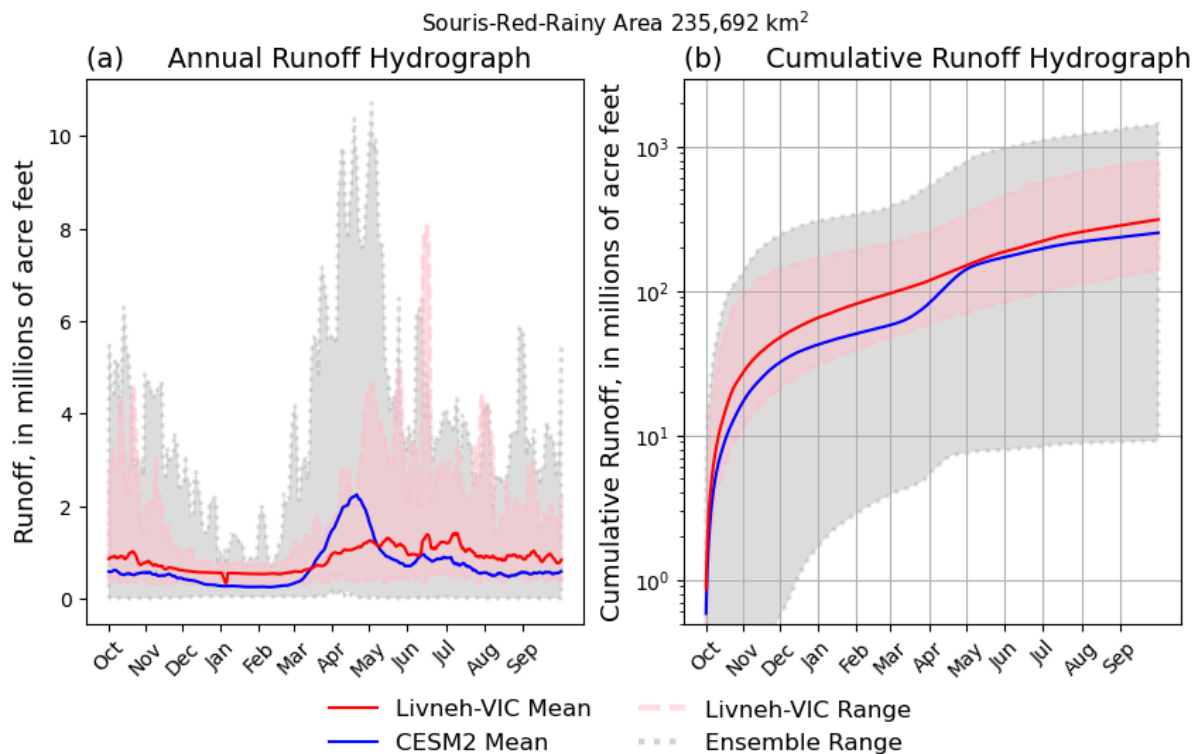
301

302 However, water management decisions are made over watersheds in units such as acre-feet<sup>1</sup> or cubic meters,  
 303 while model data are output as a depth of runoff over each grid cell (e.g., mm/day per km<sup>2</sup>). We aggregated the  
 304 7-day running mean daily runoff (Q7) within each HUC2 region to generate Q7 time series in each basin. Fig.  
 305 76a illustrates the 25-year mean seasonal cycle for Livneh-VIC in red and CESM2 in blue, and the full range of  
 306 values over all years and ensemble members for the Souris-Red-Rainy basin (HUC Region 9). Data are  
 307 presented in millions of acre feet, to align with decision maker needs. The minimum simulated Q7 in any year  
 308 considerably underestimates the lowest flows in this region compared to Livneh-VIC. In contrast, the largest

309 <sup>1</sup> 1 Acre-foot is the volume of water it would take to cover 1 acre of land to a depth of 1 foot. Equal to 325,852  
 310 gallons or 1,233 m<sup>3</sup> (USGS Water Science).



311 total runoff volume is overestimated and peaks too early in the water year. Figure 76b plots the same  
 312 information as the cumulative runoff volume from the start of the water year, highlighting that the lowest runoff  
 313 volume is underestimated by a factor of ten. Low runoff volumes were typically underestimated in smaller  
 314 regions (e.g., NE, TN). High runoff volumes were only underestimated in three regions (LM, ARK, GUL) and  
 315 considerably overestimated in seven regions. Snow-dominated regions perform particularly poorly for both  
 316 QMax and QMin as snowpack and the timing of associated runoff are not well simulated. Transitional regions  
 317 that straddle both snow- and rain-dominated hydrology also fail to capture QMax, but better estimate Qmin (not  
 318 shown). Only the South Atlantic region reproduces both QMax and QMin.



319

320 **Figure 76: Interannual variability in runoff in Souris Red Rainy Region for a) the mean seasonal cycle; and b) the**  
 321 **cumulative watershed runoff over the water year. Livneh-VIC climatological mean in red, range of all years in pink;**  
 322 **CISM2 ensemble mean in blue and ensemble range in gray. Figure highlights the underestimation of the lowest**  
 323 **runoff volume by CISM2 by a factor of ten.**

324

325 We explored the relationship between the highest and total annual runoff (QMax/QTot), and lowest and total  
 326 annual runoff (QMin/QTot). Some regions performed well for QMax/QTot, others performed better for  
 327 QMin/QTot but there was no consistent relationship that could be utilized by decision makers.

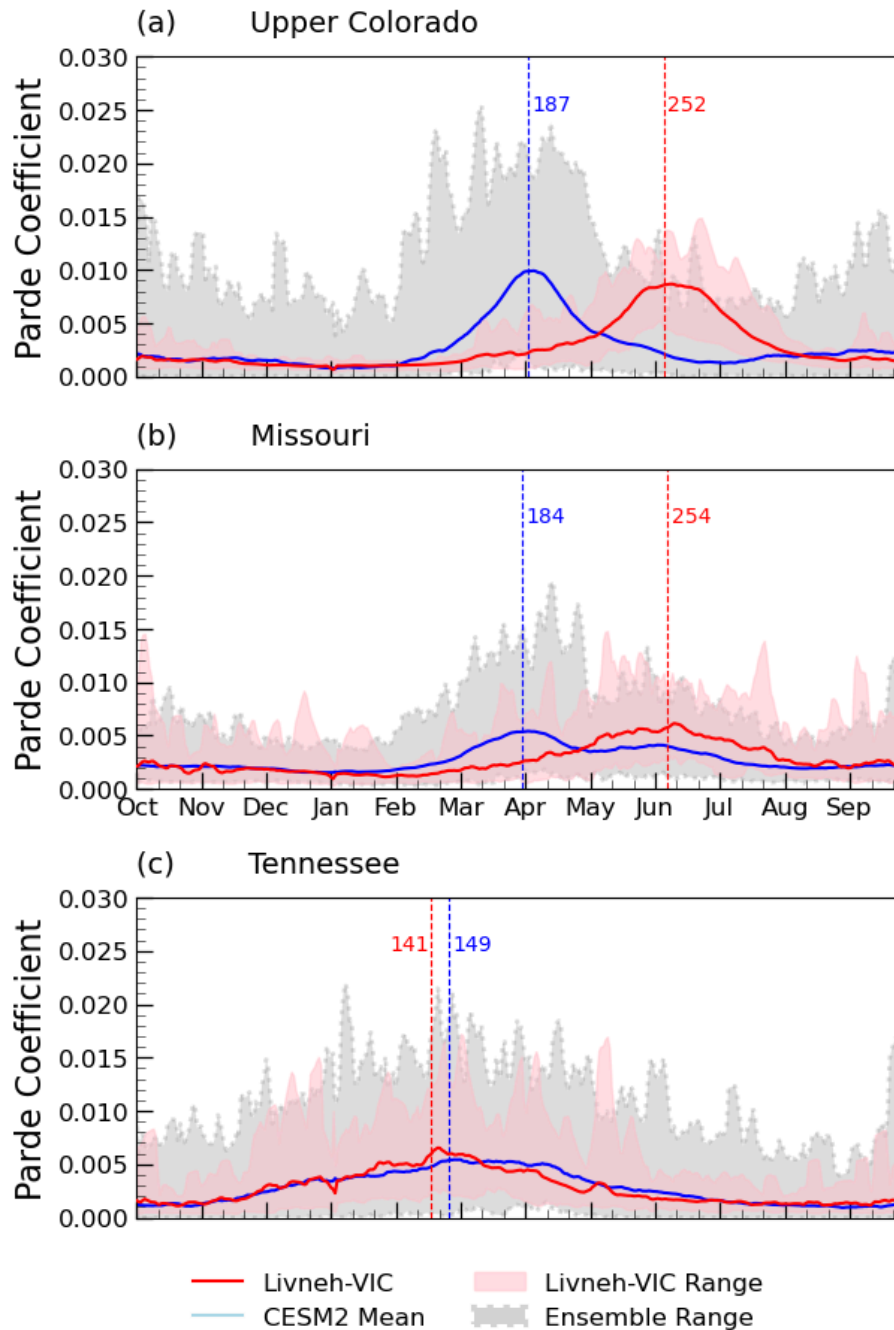
328

329 Participants at the NCAR workshop (Tye, 2023) emphasized that the exact numbers produced by climate models  
 330 are not very important for future decisions. ~~Credible interannual variability and sensitivity to change signals are~~  
 331 ~~more important to give confidence in the direction of future changes (Lehner et al., 2019).~~ Others have also  
 332 emphasized the importance of well-represented processes in the model (Reed et al., 2022) and correlations with  
 333 known experiences (Mach et al., 2020; Shepherd et al., 2018). Focussing on fidelity to the historical climate  
 334 exaggerates the importance of model performance instead of robustness to different conditions without ensuring

335 that model predictions are useful or reliable (Brunner et al., 2021; Wagener et al., 2022). Runoff estimates in  
336 transitional catchments may be inadequate in the current climate but plausible in the future, if the model  
337 reproduces rain-dominated hydrological processes (McMillan, 2021).

338

339 Climatological mean runoff cycles are estimated from Pardé coefficients — calculated as  $Q7/Q_{Tot}$  on each  
340 calendar day — a dimensionless value that enables comparison across regions. Figure 87 depicts the mean  
341 seasonal cycle for representative snow-dominated (Upper Colorado), transitional (Missouri) and rain-dominated  
342 (Tennessee) regions, demonstrating how an imperfect representation of snow in the Upper Colorado results in  
343 CESM2 peak runoff occurring two months earlier than Livneh-VIC (Fig. 87a). The runoff regimes display very  
344 different seasonal characteristics, with CESM2 having a “mid late spring” runoff regime rather than  
345 Livneh-VIC’s “extreme early summer” regime (Fig. 87a; Haines et al., 1988). Peak runoff is also too early in  
346 transitional regions, but closer to Livneh-VIC than in snow-dominated regions (Fig. 87b). Rain-dominated  
347 regions capture both the timing of  $Q_{Max}$  and overall seasonal hydrograph shape (Fig. 87c).



348

349 **Figure 87** : Seasonal patterns of runoff for HUC2 regions a) Upper Colorado (UC); b) Tennessee (TN);  
 350 and c) Missouri (MR). Constructed from normalized series of the ratio of 7-day mean runoff to the mean annual  
 351 total. Livneh-VIC runoff climatological mean (red), climatological range (pink), CISM2 ensemble mean (blue) and  
 352 ensemble range (gray with dashed border). Vertical lines indicate the mean date of peak runoff with number of days  
 353 since the start of the water year.

354 7Q10 and 7Q90 are estimated empirically from annual minima and maxima as occurring once per decade.  
 355 Projected changes in the frequency of very low or very high-(high) runoff volumes are deemed credible where  
 356 CISM2 replicates the standard deviation of annual minima and maxima according to a  $\chi^2$  test at the 5%  
 357 significance level. Table 1 reports CISM2 and Livneh-VIC regional estimates of 7Q10 and 7Q90 and standard  
 358 deviations of the annual maxima and minima series; values in bold indicate where estimates are statistically

359 similar. It should be noted that the values in Table 1 have  $\leq 10\%$  of occurring in any year, and so represent the  
 360 tails of the runoff distribution.

361

362 **Table 1 : Very low (7Q10) and very high (7Q90) regional runoff, and standard deviation in regional annual minima ( $\sigma$**   
 363 **QMin) and annual maxima ( $\sigma$  QMax) for Livneh and CESM2. Values in bold indicate where CESM2 and**  
 364 **Livneh-VIC regional runoff are statistically similar according to a  $\chi^2$  test.**

Region		Livneh-VIC				CESM2			
		7Q10	7Q90	$\sigma$ QMin	$\sigma$ QMax	7Q10	7Q90	$\sigma$ QMin	$\sigma$ QMax
NE	1	4.1	132.4	1.3	25.5	8.6	215.1	4.7	39.9
MA	2	<b>6.9</b>	103.5	<b>2.5</b>	25.7	<b>7.4</b>	220.7	<b>3.6</b>	47.9
SA	3	<b>21.1</b>	<b>240.4</b>	<b>8.4</b>	<b>50.7</b>	<b>20.5</b>	<b>258.6</b>	<b>11.9</b>	<b>45.8</b>
GL	4	<b>6.9</b>	122.5	<b>2.2</b>	23.8	<b>7.8</b>	331.0	<b>4.3</b>	58.0
OH	5	<b>7.8</b>	187.6	<b>2.3</b>	53.0	<b>9.4</b>	260.9	<b>4.5</b>	56.4
TN	6	2.1	<b>90.5</b>	0.8	<b>23.1</b>	0	<b>98.7</b>	0.3	<b>21.7</b>
UM	7	2.1	78.2	1.7	16.9	7.9	122.3	4.7	31.5
LM	8	3.9	212.2	1.1	36.1	8.0	81.0	5.1	14.7
RR	9	1.0	<b>24.3</b>	0.5	<b>7.1</b>	0	<b>33.0</b>	0.1	<b>8.4</b>
MR	10	2.3	103.0	1.6	28.1	5.2	147.4	4.2	30.4
ARK	11	2.2	130.5	0.7	36.2	3.2	93.9	4.5	18.1
GUL	12	1.5	99.1	0.5	35.5	1.3	70.7	2.8	16.7
RIO	13	<b>0.5</b>	<b>22.5</b>	<b>0.2</b>	<b>5.8</b>	<b>0.4</b>	<b>29.5</b>	<b>1.3</b>	<b>7.3</b>
UC	14	0.6	27.3	0.2	7.2	0	74.7	0.2	15.3
LCO	15	0.5	19.4	0.2	7.5	0.3	46.7	0.7	11.6
GB	16	0.7	33.3	0.3	10.3	1.8	71.5	1.3	21.1
PN	17	20.6	266.5	7.9	50.2	4.4	449.6	2.6	87.3
CA	18	1.6	323.2	0.4	101.9	1.3	233.4	1.1	61.3

365

366 Grid-scale estimates such as mean daily runoff readily highlight why decision makers have low confidence in  
 367 CESM2 output: the metrics are not salient and appear to have no skill. After aggregating the 7-day mean daily  
 368 runoff to watershed scales, some skill emerges in the annual minima and maxima, and seasonal cycles.  
 369 Snow-dominated watersheds perform poorly with regard to peak runoff volume and timing of the peaks and  
 370 lows, as expected (McCrary et al., 2022). Rain-dominated watersheds capture the inter-annual variability and  
 371 magnitudes of peak and low flows, and the seasonal hydrographs. While CESM2 at this coarse scale does not

372 represent the local topography and cannot represent finer scale snow, our analysis indicates the land surface  
373 model correctly simulates the overall bulk water budget for most watersheds as illustrated in Figures 7 and 8.  
374 However, the tail behavior of highest and lowest total watershed runoff is only captured by a few basins and so  
375 caution needs to be exercised in the interpretation and use of model results, as biases may propagate into the  
376 future. ~~The projected runoff responses in regions that will have little to no snow in the future are, therefore,~~  
377 ~~credible.~~ This is premised on the understanding of *why* the model can produce accurate results, and whether the  
378 accuracy can be reliably reproduced for the future climate (Wagener et al., 2022).

## 379 ~~5~~ ~~Projected Changes~~

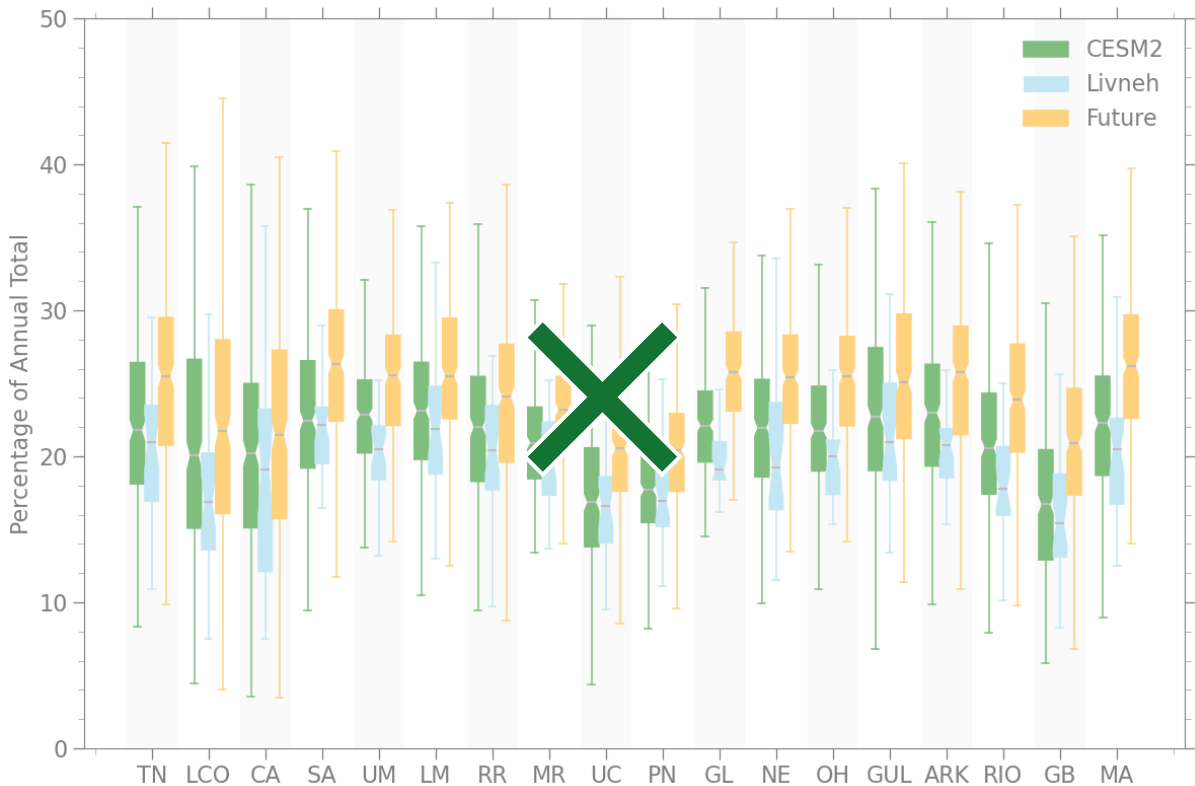
380 ~~The analyses presented in Section 4 identified some rainfall and runoff metrics salient to water resource~~  
381 ~~managers, and well-capture by CESM2.~~ While participants at the NCAR workshop stated that precise estimates  
382 are not necessary, they also emphasized their desire for high confidence in the projected scale and direction of  
383 any changes. We note that “confidence” is derived from a combination of 1) credible process representation; 2)  
384 agreement with historical trends, given internal variability; 3) agreement across multiple models. It is worth  
385 noting that trends in extremes may be important without being statistically significant, as a limited sample of  
386 points (e.g. one per year) from a stochastic series is inherently noisy. However, some of these trends may  
387 emerge from the noise in the distribution and so are important to monitor. ~~As the scope of this research was~~  
388 ~~limited to testing the first aspect, we present projections for precipitation and runoff metrics in the nine regions~~  
389 ~~where CESM2 is credible.~~

### 390 ~~5.1~~ ~~Rainfall metrics~~

391 ~~Projected precipitation metrics suggest no statistically significant changes in the frequency of wet days (NWD)~~  
392 ~~in any region by mid-century under the SSP2 4.5 emissions scenario. Mean seasonal precipitation is projected to~~  
393 ~~increase in New England (NE) and Pacific Northwest (PN) during winter and spring, but overall changes are~~  
394 ~~slight. However, minor changes in the mean obscure the projected increasing intensity of the heaviest~~  
395 ~~precipitation days and persistence of dry or wet spells (Donat et al., 2019).~~

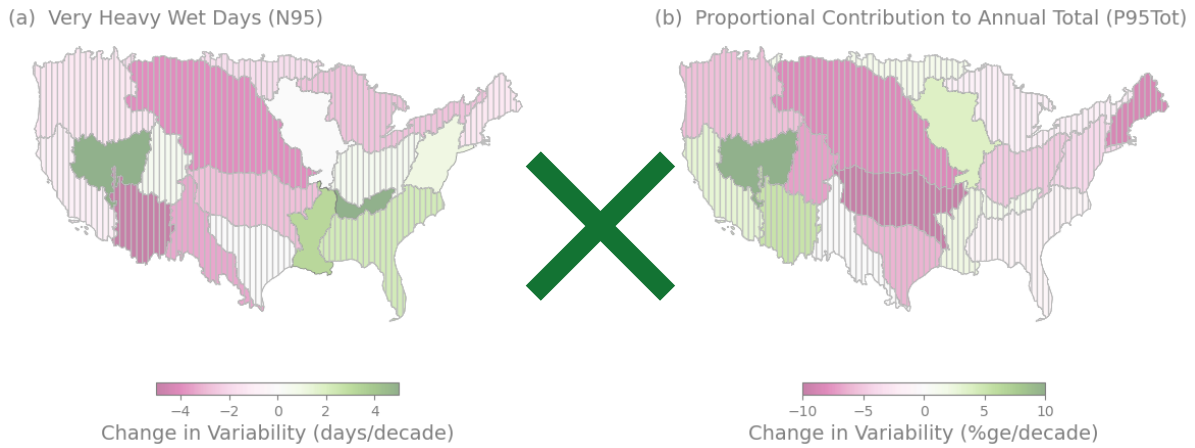
396 ¶

397 ~~Figure 9 compares the range of contributions to the annual total from very heavy rain days (P95Tot). The bars~~  
398 ~~encapsulate the interquartile range of all years per region with black bars at the median of all years for Livneh~~  
399 ~~(blue) and all years and all ensemble members for CESM2 (green and orange); whiskers show the full extents of~~  
400 ~~the data. Well-performing regions have the greatest overlaps between green (CESM2) and blue (Livneh) bars,~~  
401 ~~while overlapping notches indicate statistical similarity. All regions show projected increases in the volume of~~  
402 ~~annual total precipitation that will derive from the most extreme events, with significant changes indicated by~~  
403 ~~divergent notches between green and orange (Future). Some regions (e.g., LCO, UM, GB) also show increasing~~  
404 ~~volatility of wetter or drier years, as indicated by longer whiskers and/or bars.~~



405  
 406 ~~Figure 8: Box plots of the interannual range of contributions to annual total rainfall from very heavy days (P95Tot)~~  
 407 ~~shown as percentages for: Livneh 1981-2010 (light blue), and also ensemble ranges for CESM2 1981-2010 (green) and~~  
 408 ~~CESM2 2040-2070 (orange) for all HUC2 regions. Boxes are bound by the interquartile range, black lines indicate the~~  
 409 ~~median, and bars extend to the full data range.~~

410  
 411 ~~Interannual variability is illustrated further for N95 (Fig. 9a) and P95Tot (Fig. 9b). Regions that are not~~  
 412 ~~statistically significant (for a student's t-test at 5% significance) are hatched. Both plots indicate the majority of~~  
 413 ~~basins in the west will experience a decrease (albeit statistically insignificant) in the interannual variability of~~  
 414 ~~N95 and their intensity. Great Basin (GB) is notable in projecting a significant increase in both the interannual~~  
 415 ~~variability in N95, and their intensity. This reduction in predictability could exacerbate existing water resource~~  
 416 ~~problems, and have potential consequences for the downstream basins (LCO, CA).~~  
 417 ¶



418

419 **Figure 9. CESM2 ensemble mean projected changes in interannual variability in a) frequency of very heavy wet days**  
 420 **and units of days per decade, and b) proportional contribution to the annual total and units of percent per decade.**  
 421 **Hatching indicates the region does not reach statistical significance. ¶¶**

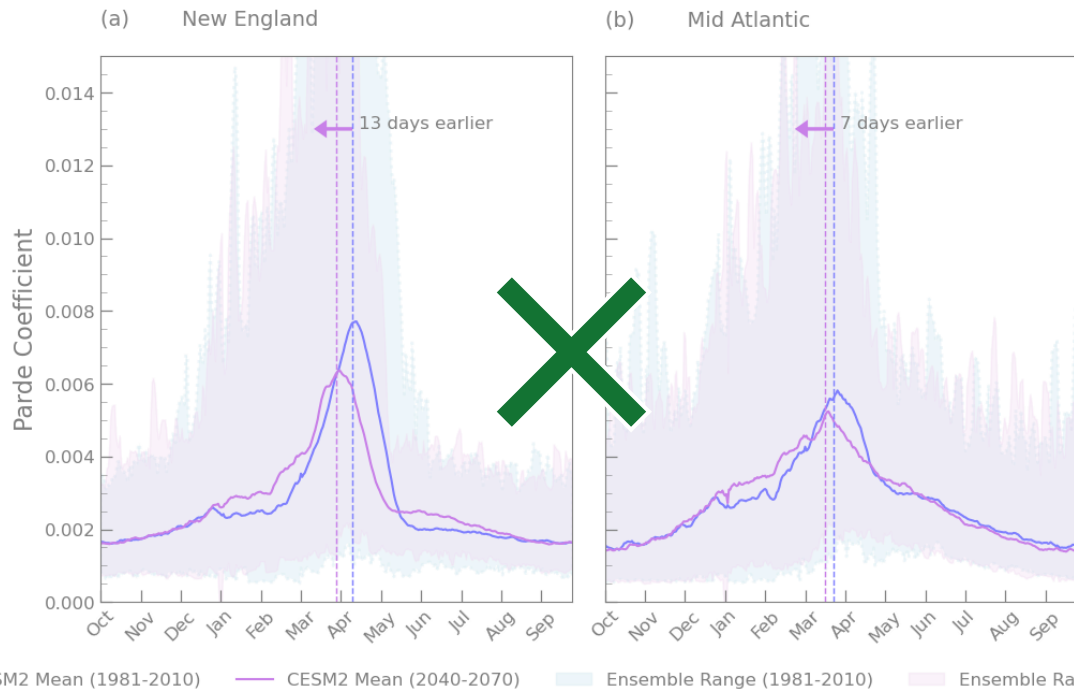
422 California is projected to halve the frequency of very heavy days, but the proportional contribution of those days  
 423 to the annual total will increase from 20% to 22% (Fig. 8). This is coupled with projected increases in variability  
 424 in the frequency and intensity of the heaviest events (Fig. 9), and reduced persistence in the duration of wet and  
 425 dry spells (not shown). While not all of these changes are statistically significant, they are consistent with results  
 426 from higher resolution models and suggest an increased potential for fire weather, drought, and floods (Lukas  
 427 and Payton, 2020; Reclamation, 2016). Similar narratives are found for other regions, with several showing  
 428 significant changes in the swings from wet to dry years (Fig. 9a). This emphasizes the importance of examining  
 429 multiple precipitation metrics, and working with local partners to highlight potential risks and develop the full  
 430 storyline of how future water management decisions relate to their experience.

431 **5.2 Runoff metrics ¶¶**

432 CESM2-LENS projections could helpfully augment RCM higher resolution model output in rain-dominated  
 433 regions such as Tennessee, Ohio, and California, where CESM2 most closely reproduces Livneh-VIC, by  
 434 providing supplementary information on the relative uncertainty in the models. This is also true for transitional  
 435 basins such as the Rio Grande, Northeast, and Lower Colorado, where seasonal snowpack may become more  
 436 ephemeral and change the seasonal hydrological responses.

437

438 Based on the mean day of QMax, identified from Pardé coefficients, CESM2 projects QMax will occur around 5  
 439 days earlier in Tennessee, Ohio, and California by 2070 (Fig. 10). The duration of low flows at the end of the  
 440 water year may also increase by around 5 days (not shown), but additional analysis using all CESM2-LENS  
 441 members is needed to determine the true signal-to-noise in low-flow durations (Lehner et al., 2017). Transitional  
 442 regions may experience QMax up to two weeks earlier as a result of changes in precipitation type. ¶¶



443 — CSM2 Mean (1981-2010) — CSM2 Mean (2040-2070) — Ensemble Range (1981-2010) — Ensemble Range (2040-2070) ¶

444 ~~Figure 10: Example of projected changes in seasonal runoff timing for regions a) New England (NE);~~  
 445 ~~and b) Mid-Atlantic (MA).~~ ¶

446 ¶

447 ~~The projected frequency of 7Q90 and 7Q10 has potential skill in CESM2 that would benefit water resource~~  
 448 ~~managers. The projected changes in seasonal and multi-year behavior point to increases in the east-west divide~~  
 449 ~~in drought-related problems. California is projected to have little change in 7Q90 frequency that may generate~~  
 450 ~~floods but twice the frequency of very low events, while the South Atlantic may double or triple 7Q90~~  
 451 ~~frequency with little change in 7Q10 frequency. Table 2 compares the projected changes in frequencies of 7Q90~~  
 452 ~~and 7Q10 events between 2040-2070 and 1981-2005. Effective change is calculated from the difference in~~  
 453 ~~ensemble mean of the expected rates over thirty years (i.e. 3 events in the current period). Color coding indicates~~  
 454 ~~a subjective human-impacts assessment of beneficial (green) or adverse (orange) changes. Both 7Q90 and 7Q10~~  
 455 ~~can have benefits from an ecological perspective and so no change is the most beneficial condition. However,~~  
 456 ~~the built environment is designed to be “fail-safe” (Tye et al., 2015) such that a lower probability of flooding~~  
 457 ~~would be beneficial, and restrictions on water availability would be adverse.~~ ¶

458 ¶

459 ~~Table 2: Projected changes in the frequency of very high flows (7Q90) and very low flows (7Q10) per decade for~~  
 460 ~~well-simulated regions. Color coding indicates beneficial (green) or adverse (orange) changes in runoff regimes~~ ¶

Region ¶	7Q90-per-decade ¶	Effective-Change ¶	7Q10-per-decade ¶	Effective-Change ¶
(1) NE ¶	0.4 ¶	-1.0 ¶	1.1 ¶	0 ¶
(10) MR ¶	0.2 ¶	-1.0 ¶	2.0 ¶	+1.0 ¶
(18) CA ¶	0.8 ¶	0 ¶	2.4 ¶	+1.0 ¶
(2) MA ¶	0.6 ¶	0 ¶	1.2 ¶	0 ¶
(3) SA ¶	3.3 ¶	+2.0 ¶	1.0 ¶	0 ¶
(5) OH ¶	1.0 ¶	0 ¶	0.8 ¶	0 ¶



Region	<del>7Q90 per decade</del>	Effective Change	<del>7Q10 per decade</del>	Effective Change
(6) TN	<del>2.0</del>	+1.0	<del>2.0</del>	+1.0
(9) RR	<del>1.0</del>	0	<del>3.4</del>	+2.0

461 **6 Discussion**

462 As decision makers have become more immersed in developing water resource management adaptation plans,  
 463 the role of “climate services” in developing salient climate information has increased (Briley et al., 2020;  
 464 Brugger et al., 2016; Dilling et al., 2019). We tested our hypothesis that recent improvements in ESMs can allow  
 465 decision-relevant metrics to be produced directly, by leveraging the combined experience of the author team,  
 466 results from the NCAR workshop, and the wealth of literature on actionable knowledge (Bremer et al., 2020;  
 467 Jagannathan et al., 2021; Mach et al., 2020; Vano et al., 2014). Given that no model can perfectly address all  
 468 decision needs, we identified and evaluated multiple metrics that can frame specific water management  
 469 decisions within the known constraints of the data (Lempert, 2021), or within the decision makers’ experiences  
 470 (Austin, 2023; Clifford et al., 2020; Reed et al., 2022; Shepherd et al., 2018).

471

472 It is important to communicate the original purpose of the model and associated weaknesses, so that decision  
 473 makers fully understand which information is appropriate to use in other applications (Fisher and Koven, 2020;  
 474 Gettelman and Rood, 2016; Wagener et al., 2022). Given the balance between model fidelity and model  
 475 complexity (Clark et al., 2015) and the absence of detailed global scale observation data (e.g., Gleason and  
 476 Smith, 2014; Reba et al., 2011) CESM2 provides a plausible representation of Earth system processes and  
 477 moisture fluxes, but may not capture basin-scale specifics (Ek, 2018; Lehner et al., 2019). That said, there are  
 478 continued efforts to improve the simulation of land surface processes and analyses such as those presented in  
 479 this article can flag weaknesses for future improvement (Lawrence et al., 2019).

480

481 Establishing model fidelity also requires distinguishing an accurate representation of the climate processes from  
 482 serendipitous correlation with observations. Whether the model has good process representation overall, or  
 483 exactitude in one simulation can be established through internal variability analyses using large ensembles (e.g.,  
 484 Deser et al., 2020; Tebaldi et al., 2021). Repeating the analyses with several different ESMs to establish the  
 485 degree of agreement (Mankin et al., 2020) would further strengthen the usability of metrics presented in this  
 486 article. It is also worth noting that the analysis presented here only used one reference dataset. As different  
 487 reanalysis and observational datasets can have large discrepancies, a thorough model evaluation would also  
 488 benefit from comparison to several products (Kim et al., 2020; Newman et al., 2015), *including an assessment*  
 489 *of how removing temporal adjustments in observations affects the statistics of extremes (Pierce et al., 2021).*

490

491 While the precise details of precipitation and runoff may not be well simulated by CESM2, we found some  
 492 aspects are ~~sufficiently credible to support decision needs~~. The frequency of wet days highlighted regions where  
 493 current seasonal behavior is well captured, and ~~may future behavior is plausible enough to support planning~~  
 494 around flood and drought control or wildfire risk *when used in combination with other models or data sources*

495 (Austin, 2023; Clifford et al., 2020; Jagannathan et al., 2021; Reclamation, 2016). ~~CESM2 projects increases in~~  
496 ~~late spring and early fall rain, instead of snow, and in the longest wet and dry spells affecting soil moisture~~  
497 ~~capacity and the tendency for episodic floods and droughts in common with other basin-wide assessments (e.g.,~~  
498 ~~Lukas and Payton, 2020; Underwood et al., 2018). Our analyses are also consistent with higher-resolution model~~  
499 ~~projections of increases in the most extreme rainfall events (Fowler et al., 2021).~~

## 500 7 Conclusions

501 This paper presented an assessment of whether a standard resolution (~100 km grid) Earth system model is  
502 capable of producing information that water users typically employ in their decisions. Our motivation was to  
503 explore whether it is possible to reduce the need for intermediate downscaling, and to broaden the use of large  
504 model ensembles to quantify the influence of internal variability on localized decisions. We drew on the  
505 combined experience of the project team and workshop participants to identify potential metrics and familiar  
506 modes of visualization. This project used only CESM2 over the conterminous United States to develop example  
507 metrics that may be explored within other models and over other regions. ~~CESM2 is unable to reproduce some~~  
508 ~~metrics given the lack of topographical detail. A companion paper by Rugg et al. (2023) examines potential~~  
509 ~~improvements to the subgrid-scale simulation of land processes to improve the representation of the~~  
510 ~~hydrological cycle in mountainous regions.~~

511

512 ~~Given the inherent limitations of large-scale models in replicating small-scale processes, we only presented~~  
513 ~~future projections for regions where processes are well-resolved on the coarse grid. We encourage others~~  
514 ~~working in the decision space between climate data producers and users to be forthcoming about specific~~  
515 ~~regions and reasons where model data are not credible, or where the model has particular weaknesses (such as~~  
516 ~~the drizzle effect) that may be overcome with a different analysis approach.~~

517 For future model assessors, the following metrics were found to be salient for water users and were skillfully  
518 reproduced in many regions.

519

520 Rainfall:

- 521     ▪ Number of wet days ( $\geq 1$ mm of rain) per year/season
- 522     ▪ Mean precipitation on wet days
- 523     ▪ Duration of the longest wet and dry spells per year
- 524     ▪ Number of days with rain  $>$  95th percentile of current climate wet day totals
- 525     ▪ Proportion of the annual total derived from days  $>$  95th percentile of wet day totals

526 Runoff (aggregated up to basin level, as a volume for 3- and 7-day averages):

- 527     ▪ Annual maxima and minima

528     ▪   Frequency of very high or very low flows (< 10% annual chance of occurring in the current climate)

529     ▪   Proportion of averaged daily runoff to annual total

530

531 The work presented in this paper is a small step toward establishing greater usability of climate model output by  
 532 decision makers. Continued collaboration is essential to improve the transfer of knowledge (e.g., data  
 533 requirements, model assumptions, decision constraints) between communities.

534

535 **Appendix A**

536

537 **Table A1: Hydro-meteorological responses used in water management decisions, and the specific metrics that have**  
 538 **potential for representation in ESMs. Metrics in bold are presented in this article.**

<b>Hydro-meteorological Responses</b>	<b>Typical Water Management Decision</b>	<b>Metric</b>	<b>Description</b>
Annual rainfall	Water supply and drought monitoring	Total Precipitation (PRCPTOT)	Total annual precipitation measured as rainfall or snow water equivalent.
Seasonal rainfall cycle	Seasonal water supply, reservoir operations management	Number of Wet Days (NWD), Mean Wet Day Volume (WDV)	Frequency of days with $\geq 1$ mm precipitation (NWD) per month, season or year, Mean precipitation on wet days calculated from PRCPTOT/NWD
Rainfall extreme	Flood and stormwater management	95th percentile (Q95) Number of very heavy rain days (N95) Very heavy rain volume (P95) Proportional contribution of very heavy rain (P95tot)	Rainfall percentile threshold that is exceeded by 5% rain events per year on average, and calculated from wet days only Frequency of days with rainfall exceeding Q95 Total rain falling on days exceeding Q95 Proportional of annual total derived from very heavy rain, calculated as P95/PRCPTOT
Rainfall extreme (dry)	Water supply planning and drought monitoring/planning including water rights and restrictions.	Consecutive dry days (CDD)	Maximum duration of spell with consecutive days measuring < 1 mm precipitation.

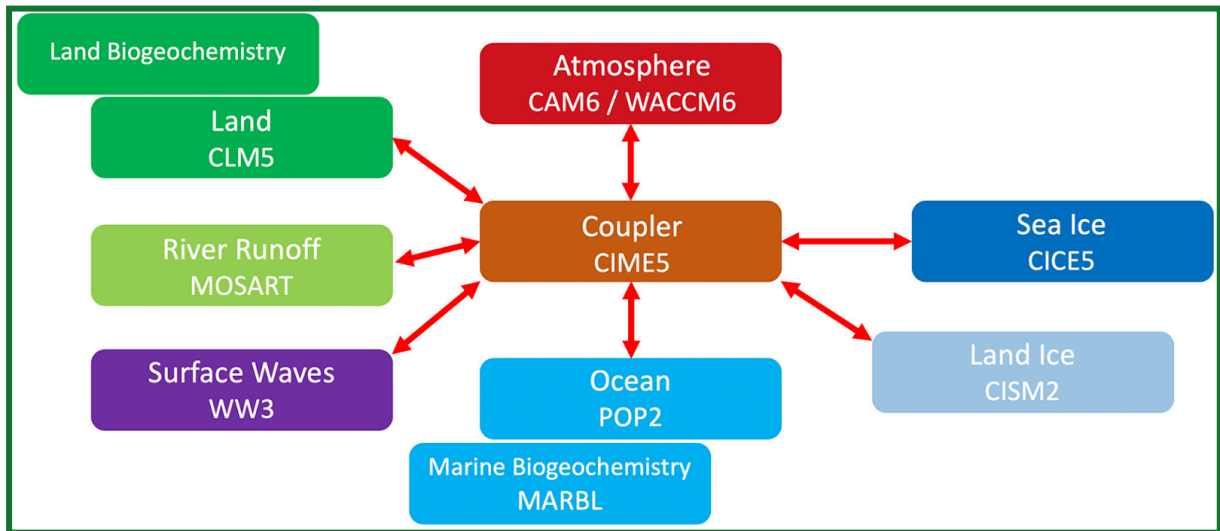
<b>Hydro-meteorological Responses</b>	<b>Typical Water Management Decision</b>	<b>Metric</b>	<b>Description</b>
Rainfall extreme (wet)	Stormwater management, water supply planning	Consecutive wet days (CWD)	Maximum duration of spell with consecutive days measuring $\geq 1$ mm precipitation.
High streamflow	Reservoir management and flood control, water quality management and water supply management, including use of supplemental water supplies	Annual maximum runoff (QMax) Description (JMaxF) Description (HFD)	Annual maximum daily volume of basin-wide runoff Julian day of QMax/ day of the water year Duration of high flows
Low streamflow	Water supply management, assessment of water shortages with respect to seasonal demands	Annual minimum runoff (QMin) Description (JMinF) Description (LFD)	Annual minimum daily volume of basin-wide runoff Julian day of QMin/ day of the water year Duration of low flows
Streamflow	Water supply planning, water quality management, reservoir operations management, planning future investment needs	7-day mean runoff (Q7)	Daily volume of basin-wide runoff averaged over 7 days. Often presented as percentage of annual total volume of runoff or Pardé coefficient (Pardé, 1933)
Very low streamflow	Water quality management for discharge permits, conservation management, drought planning	7-day "10-year" low runoff (7Q10)	7-day averaged basin-wide lowest volume of runoff with <10% annual probability of occurring. Estimated from Qmin series.
Very high flow	Flood management and planning, reservoir operations	7-day "10-year" high runoff (7Q90)	7-day averaged basin-wide highest volume of runoff with <10% annual probability of occurring. Estimated from Qmax series.
Streamflow	Water supply planning, reservoir operations management	Central Tendency (CT) Description (Q <sub>25</sub> , Q <sub>50</sub> , Q <sub>75</sub> )	Day of the water year when the cumulative annual runoff exceeds 50% of the total annual runoff

<b>Hydro-meteorological Responses</b>	<b>Typical Water Management Decision</b>	<b>Metric</b>	<b>Description</b>
			Annual quartiles of cumulative annual runoff estimated from daily streamflow.
Snowpack	Reservoir operations and flood management, water supply planning	Snow Water Equivalent (SWE) Maximum (SWEMax) SWEMax Date SWE Duration	Volume of peak snow water equivalent Day of the water year when peak SWE occurs Total length of snow accumulation and ablation
Snowmelt	Flood management and reservoir operations	Snowmelt onset	Day of water year of snowmelt onset

539

540 **Appendix B**

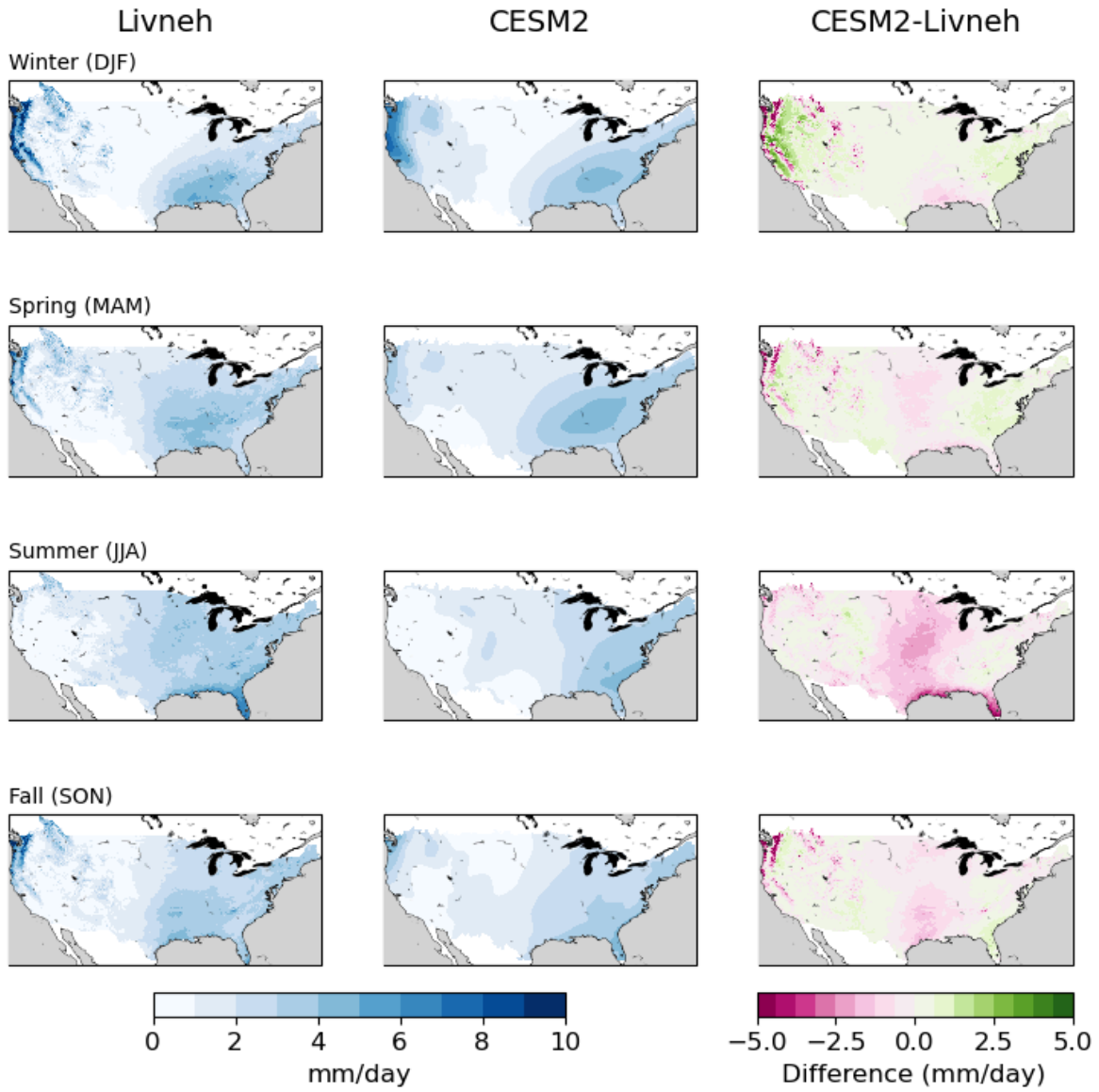
541 Schematic of the Community Earth System Model version 2 (CESM2) model components, reproduced from  
542 Danabasoglu et al. (2020) Figure 1.



543

544 **Appendix CB**

545 Seasonal Mean Precipitation for Winter (top row), Spring (row 2), Summer (row 3) and Fall (bottom row) as shown  
546 in Livneh (left column) and CESM2 (middle column), and difference CESM2-Livneh (right column)

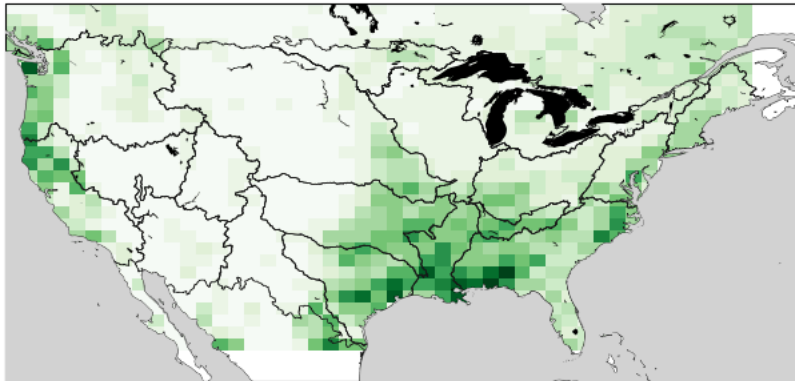


547

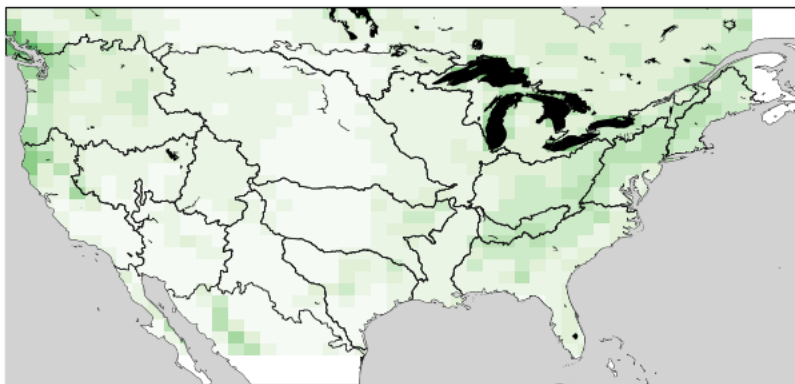
548

### Maximum Daily Runoff (1981-2005)

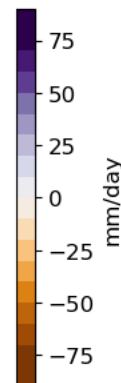
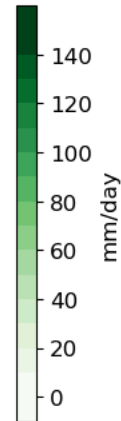
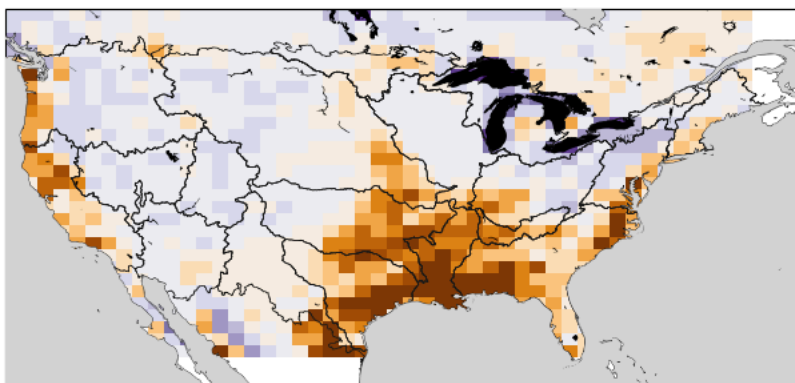
(a) Observations (Livneh-VIC)



(b) CESM2



(c) Difference (CESM2 - Livneh-VIC)





## 554 Data availability

555 All data generated for this study (e.g., CESM2 and Livneh-VIC calculated indices) along with Jupyter  
556 notebooks to recreate tables and figures are available in the repository  
557 [https://github.com/maritye/PSIF\\_water\\_avail](https://github.com/maritye/PSIF_water_avail)

## 558 Author Contribution

559 Conceptualization, M.T., J.R., E.G., A.N., A.W. and R.M.; Methodology, M.T., J.R., E.G.; Investigation, M.G.,  
560 M.T.; Data Curation, M.G., M.T.; Writing - original draft, M.T., A.R., and R.M.; Writing – reviewing and  
561 editing, M.T., J.R., E.G., A.N., A.W., R.M., A.R., F.L., C.B., and S.H.; Visualization, C.B., M.G. and M.T.;  
562 Supervision, J.R., E.G., A.N., F.L. and A.W.; Funding Acquisition, J.R., E.G., A.N., A.W., F.L., C.B., S.H. and  
563 M.T.; Project Administration J.R.

## 564 Competing Interests

565 The authors declare that they have no conflict of interest.

## 566 Acknowledgements

567 This material is based upon work supported by the National Center for Atmospheric Research (NCAR), which is  
568 a major facility sponsored by the National Science Foundation (NSF) under Cooperative Agreement No.  
569 1852977. Computing resources were provided by the Climate Simulation Laboratory at NCAR’s Computational  
570 and Information Systems Laboratory (CISL). The CESM project is supported primarily by NSF. We thank all  
571 the scientists, software engineers, and administrators who contributed to the development of CESM2. For the  
572 CESM2 Large Ensemble output we thank the CESM2 Large Ensemble Community Project and the  
573 supercomputing resources provided by the IBS Center for Climate Physics in South Korea. This research was  
574 primarily supported by the UCAR President’s Strategic Initiative Fund. Portions of this study were supported by  
575 the Regional and Global Model Analysis (RGMA) component of the Earth and Environmental System  
576 Modeling Program of the U.S. Department of Energy’s Office of Biological & Environmental Research (BER)  
577 under Award Number DE-SC0022070.

## 578 References

579 ASCE: Standard Guidelines for the Design of Urban Stormwater Systems, Standard Guidelines for Installation  
580 of Urban Stormwater Systems, and Standard Guidelines for the Operation and Maintenance of Urban  
581 Stormwater Systems, 45th ed., American Society of Civil Engineers, Reston, VA,  
582 <https://doi.org/10.1061/9780784408063>, 2006.  
583 Jeanine Jones: Drought and lessons learned:  
584 <https://mavensnotebook.com/2023/03/01/jeanine-jones-drought-and-lessons-learned/>, last access: 2 May 2023.  
585 Bachmair, S., Stahl, K., Collins, K., Hannaford, J., Acreman, M., Svoboda, M., Knutson, C., Smith, K. H., Wall,  
586 N., Fuchs, B., Crossman, N. D., and Overton, I. C.: Drought indicators revisited: the need for a wider  
587 consideration of environment and society, WIREs Water, 3, 516–536, <https://doi.org/10.1002/wat2.1154>, 2016.

588 Brekke, L. D.: Addressing Climate Change in Long-Term Water Resources Planning and Management: User  
589 Needs for Improving Tools and Information, Bureau of Reclamation, Technical Service Center, Denver, 2011.

590 Brekke, L. D., Kiang, J. E., Olsen, J. R., Pulwarty, R. S., Raff, D. A., Turnipseed, D. P., Webb, R. S., and White,  
591 K. D.: Climate change and water resources management—A federal perspective, U.S. Geological Survey, 2009.

592 Bremer, L. L., Hamel, P., Ponette-González, A. G., Pompeu, P. V., Saad, S. I., and Brauman, K. A.: Who Are we  
593 Measuring and Modeling for? Supporting Multilevel Decision-Making in Watershed Management, *Water*  
594 *Resources Research*, 56, <https://doi.org/10.1029/2019WR026011>, 2020.

595 Briley, L., Kelly, R., Blackmer, E. D., Troncoso, A. V., Rood, R. B., Andresen, J., and Lemos, M. C.: Increasing  
596 the Usability of Climate Models through the Use of Consumer-Report-Style Resources for Decision-Making,  
597 *Bulletin of the American Meteorological Society*, 101, E1709–E1717,  
598 <https://doi.org/10.1175/BAMS-D-19-0099.1>, 2020.

599 Brugger, J., Meadow, A., and Horangic, A.: Lessons from First-Generation Climate Science Integrators, *Bulletin*  
600 *of the American Meteorological Society*, 97, 355–365, <https://doi.org/10.1175/BAMS-D-14-00289.1>, 2016.

601 Brunner, M. I., Slater, L., Tallaksen, L. M., and Clark, M.: Challenges in modeling and predicting floods and  
602 droughts: A review, *WIREs Water*, 8, <https://doi.org/10.1002/wat2.1520>, 2021.

603 Cantor, A., Kiparsky, M., Kennedy, R., Hubbard, S., Bales, R., Pecharroman, L. C., Guivetchi, K., McCready,  
604 C., and Darling, G.: Data for Water Decision Making: Informing the Implementation of California’s Open and  
605 Transparent Water Data Act through Research and Engagement, Wheeler Water Institute, Center for Law,  
606 Energy & the Environment, UC Berkeley School of Law, Berkeley, CA., 2018.

607 Chen, D., Dai, A., and Hall, A.: The Convective-To-Total Precipitation Ratio and the “Drizzling” Bias in  
608 Climate Models, *JGR Atmospheres*, 126, e2020JD034198, <https://doi.org/10.1029/2020JD034198>, 2021.

609 Chen, M., Dickinson, R. E., Zeng, X., and Hahmann, A. N.: Comparison of Precipitation Observed over the  
610 Continental United States to That Simulated by a Climate Model, *Journal of Climate*, 9, 9, 2233–49,  
611 [https://doi.org/10.1175/1520-0442\(1996\)009<2233:COPOOT>2.0.CO;2](https://doi.org/10.1175/1520-0442(1996)009<2233:COPOOT>2.0.CO;2), 1996

612 Clark, M. P., Fan, Y., Lawrence, D. M., Adam, J. C., Bolster, D., Gochis, D. J., Hooper, R. P., Kumar, M.,  
613 Leung, L. R., Mackay, D. S., Maxwell, R. M., Shen, C., Swenson, S. C., and Zeng, X.: Improving the  
614 representation of hydrologic processes in Earth System Models, *Water Resour. Res.*, 51, 5929–5956,  
615 <https://doi.org/10.1002/2015WR017096>, 2015.

616 Clifford, K. R., Travis, W. R., and Nordgren, L. T.: A climate knowledges approach to climate services, *Climate*  
617 *Services*, 18, 100155, <https://doi.org/10.1016/j.cliser.2020.100155>, 2020.

618 Dai, A.: Precipitation Characteristics in Eighteen Coupled Climate Models, *Journal of Climate*, 19, 18 ,  
619 4605–30, <https://doi.org/10.1175/JCLI3884.1>, 2006

620 Danabasoglu, G. and Lamarque, J.-F.: Building a Better Model to View Earth’s Interacting Processes, *Eos*, 102,  
621 <https://doi.org/10.1029/2021EO155818>, 2021.

622 Danabasoglu, G., Lamarque, J. -F., Bacmeister, J., Bailey, D. A., DuVivier, A. K., Edwards, J., Emmons, L. K.,  
623 Fasullo, J., Garcia, R., Gettelman, A., Hannay, C., Holland, M. M., Large, W. G., Lauritzen, P. H., Lawrence, D.  
624 M., Lenaerts, J. T. M., Lindsay, K., Lipscomb, W. H., Mills, M. J., Neale, R., Oleson, K. W., Otto-Bliesner, B.,  
625 Phillips, A. S., Sacks, W., Tilmes, S., Kampenhout, L., Vertenstein, M., Bertini, A., Dennis, J., Deser, C.,  
626 Fischer, C., Fox-Kemper, B., Kay, J. E., Kinnison, D., Kushner, P. J., Larson, V. E., Long, M. C., Mickelson, S.,

627 Moore, J. K., Nienhouse, E., Polvani, L., Rasch, P. J., and Strand, W. G.: The Community Earth System Model  
628 Version 2 (CESM2), *J. Adv. Model. Earth Syst.*, 12, <https://doi.org/10.1029/2019MS001916>, 2020.

629 Deser, C., Knutti, R., Solomon, S., and Phillips, A. S.: Communication of the role of natural variability in future  
630 North American climate, *Nature Clim Change*, 2, 775–779, <https://doi.org/10.1038/nclimate1562>, 2012.

631 Deser, C., Lehner, F., Rodgers, K. B., Ault, T., Delworth, T. L., DiNezio, P. N., Fiore, A., Frankignoul, C., Fyfe,  
632 J. C., Horton, D. E., Kay, J. E., Knutti, R., Lovenduski, N. S., Marotzke, J., McKinnon, K. A., Minobe, S.,  
633 Randerson, J., Screen, J. A., Simpson, I. R., and Ting, M.: Insights from Earth system model initial-condition  
634 large ensembles and future prospects, *Nat. Clim. Chang.*, 10, 277–286,  
635 <https://doi.org/10.1038/s41558-020-0731-2>, 2020.

636 Dilling, L., Daly, M. E., Kenney, D. A., Klein, R., Miller, K., Ray, A. J., Travis, W. R., and Wilhelmi, O.:  
637 Drought in urban water systems: Learning lessons for climate adaptive capacity, *Climate Risk Management*, 23,  
638 32–42, <https://doi.org/10.1016/j.crm.2018.11.001>, 2019.

639 Donat, M. G., Angéilil, O., and Ukkola, A. M.: Intensification of precipitation extremes in the world’s humid and  
640 water-limited regions, *Environ. Res. Lett.*, 14, 065003, <https://doi.org/10.1088/1748-9326/ab1c8e>, 2019.

641 Ek, M. B.: Land Surface Hydrological Models, in: *Handbook of Hydrometeorological Ensemble Forecasting*,  
642 edited by: Duan, Q., Pappenberger, F., Thielen, J., Wood, A., Cloke, H. L., and Schaake, J. C., Springer Berlin  
643 Heidelberg, Berlin, Heidelberg, 1–42, [https://doi.org/10.1007/978-3-642-40457-3\\_24-1](https://doi.org/10.1007/978-3-642-40457-3_24-1), 2018.

644 Ekström, M., Gutmann, E. D., Wilby, R. L., Tye, M. R., and Kirono, D. G. C.: Robustness of hydroclimate  
645 metrics for climate change impact research, *Wiley Interdisciplinary Reviews: Water*, 5, e1288,  
646 <https://doi.org/10.1002/wat2.1288>, 2018.

647 Feng, R., Otto-Bliesner, B. L., Brady, E. C., and Rosenbloom, N.: Increased Climate Response and Earth System  
648 Sensitivity From CCSM4 to CESM2 in Mid-Pliocene Simulations, *J. Adv. Model. Earth Syst.*, 12,  
649 <https://doi.org/10.1029/2019MS002033>, 2020.

650 Fisher, R. A. and Koven, C. D.: Perspectives on the Future of Land Surface Models and the Challenges of  
651 Representing Complex Terrestrial Systems, *J. Adv. Model. Earth Syst.*, 12,  
652 <https://doi.org/10.1029/2018MS001453>, 2020.

653 Fowler, H. J., Wasko, C., and Prein, A. F.: Intensification of short-duration rainfall extremes and implications for  
654 flood risk: current state of the art and future directions, *Phil. Trans. R. Soc. A.*, 379, 20190541,  
655 <https://doi.org/10.1098/rsta.2019.0541>, 2021.

656 Gervais, M., Gyakum, J. R., Atallah, E., Tremblay, L. B., and Neale, R. B.: How Well Are the Distribution and  
657 Extreme Values of Daily Precipitation over North America Represented in the Community Climate System  
658 Model? A Comparison to Reanalysis, Satellite, and Gridded Station Data, *Journal of Climate*, 27, 5219–5239,  
659 <https://doi.org/10.1175/JCLI-D-13-00320.1>, 2014.

660 Gettelman, A. and Rood, R. B.: Usability of Climate Model Projections by Practitioners, in: *Demystifying*  
661 *Climate Models*, vol. 2, Springer Berlin Heidelberg, Berlin, Heidelberg, 221–236,  
662 [https://doi.org/10.1007/978-3-662-48959-8\\_12](https://doi.org/10.1007/978-3-662-48959-8_12), 2016.

663 Gettelman, A., Geer, A. J., Forbes, R. M., Carmichael, G. R., Feingold, G., Posselt, D. J., Stephens, G. L., van  
664 den Heever, S. C., Varble, A. C., and Zuidema, P.: The future of Earth system prediction: Advances in  
665 model-data fusion, *Sci Adv*, 8, eabn3488, <https://doi.org/10.1126/sciadv.abn3488>, 2022.

666 Haines, A. T., Finlayson, B. L., and McMahon, T. A.: A global classification of river regimes, *Applied*  
667 *Geography*, 8, 255–272, [https://doi.org/10.1016/0143-6228\(88\)90035-5](https://doi.org/10.1016/0143-6228(88)90035-5), 1988.

668 IPCC: *Climate Change 2022: Impacts, Adaptation, and Vulnerability. Contribution of Working Group II to the*  
669 *Sixth Assessment Report of the Intergovernmental Panel on Climate Change*, edited by: Pörtner, H.-O., Roberts,  
670 D. C., Tignor, M., Poloczanska, E. S., Mintenbeck, K., Alegría, A., Craig, M., Langsdorf, S., Lösschke, S.,  
671 Möller, V., Okem, A., and Rama, B., Cambridge University Press, 2022.

672 Jagannathan, K., Jones, A. D., and Ray, I.: The Making of a Metric: Co-Producing Decision-Relevant Climate  
673 Science, *Bulletin of the American Meteorological Society*, 102, E1579–E1590,  
674 <https://doi.org/10.1175/BAMS-D-19-0296.1>, 2021.

675 Jones, P. W.: First- and Second-Order Conservative Remapping Schemes for Grids in Spherical Coordinates,  
676 *Mon. Wea. Rev.*, 127, 2204–2210, [https://doi.org/10.1175/1520-0493\(1999\)127<2204:FASOCR>2.0.CO;2](https://doi.org/10.1175/1520-0493(1999)127<2204:FASOCR>2.0.CO;2),  
677 1999.

678 Kim, Y.-H., Min, S.-K., Zhang, X., Sillmann, J., and Sandstad, M.: Evaluation of the CMIP6 multi-model  
679 ensemble for climate extreme indices, *Weather and Climate Extremes*, 29, 100269,  
680 <https://doi.org/10.1016/j.wace.2020.100269>, 2020.

681 Lawrence, D. M., Fisher, R. A., Koven, C. D., Oleson, K. W., Swenson, S. C., Bonan, G., Collier, N., Ghimire,  
682 B., Kampenhout, L., Kennedy, D., Kluzek, E., Lawrence, P. J., Li, F., Li, H., Lombardozzi, D., Riley, W. J.,  
683 Sacks, W. J., Shi, M., Vertenstein, M., Wieder, W. R., Xu, C., Ali, A. A., Badger, A. M., Bisht, G., Broeke, M.,  
684 Brunke, M. A., Burns, S. P., Buzan, J., Clark, M., Craig, A., Dahlin, K., Drewniak, B., Fisher, J. B., Flanner, M.,  
685 Fox, A. M., Gentine, P., Hoffman, F., Keppel-Aleks, G., Knox, R., Kumar, S., Lenaerts, J., Leung, L. R.,  
686 Lipscomb, W. H., Lu, Y., Pandey, A., Pelletier, J. D., Perket, J., Randerson, J. T., Ricciuto, D. M., Sanderson, B.  
687 M., Slater, A., Subin, Z. M., Tang, J., Thomas, R. Q., Val Martin, M., and Zeng, X.: The Community Land  
688 Model Version 5: Description of New Features, Benchmarking, and Impact of Forcing Uncertainty, *J. Adv.*  
689 *Model. Earth Syst.*, 11, 4245–4287, <https://doi.org/10.1029/2018MS001583>, 2019.

690 Lehner, F., Deser, C., and Terray, L.: Toward a New Estimate of “Time of Emergence” of Anthropogenic  
691 Warming: Insights from Dynamical Adjustment and a Large Initial-Condition Model Ensemble, *Journal of*  
692 *Climate*, 30, 7739–7756, <https://doi.org/10.1175/JCLI-D-16-0792.1>, 2017.

693 Lehner, F., Wood, A. W., Vano, J. A., Lawrence, D. M., Clark, M. P., and Mankin, J. S.: The potential to reduce  
694 uncertainty in regional runoff projections from climate models, *Nat. Clim. Chang.*, 9, 926–933,  
695 <https://doi.org/10.1038/s41558-019-0639-x>, 2019.

696 Lempert, R. J.: Measuring global climate risk, *Nat. Clim. Chang.*, 11, 805–806,  
697 <https://doi.org/10.1038/s41558-021-01165-9>, 2021.

698 Liang, X., Lettenmaier, D. P., Wood, E. F., and Burges, S. J.: A simple hydrologically based model of land  
699 surface water and energy fluxes for general circulation models, *J. Geophys. Res.*, 99, 14415,  
700 <https://doi.org/10.1029/94JD00483>, 1994.

701 Livneh, B., Rosenberg, E. A., Lin, C., Nijssen, B., Mishra, V., Andreadis, K. M., Maurer, E. P., and Lettenmaier,  
702 D. P.: A Long-Term Hydrologically Based Dataset of Land Surface Fluxes and States for the Conterminous  
703 United States: Update and Extensions, *J. Climate*, 26, 9384–9392, <https://doi.org/10.1175/JCLI-D-12-00508.1>,  
704 2013.

705 Lukas, J. and Payton, E.: Colorado River Basin Climate and Hydrology: State of the Science,  
706 <https://doi.org/10.25810/3HCV-W477>, 2020.

707 Mach, K. J., Lemos, M. C., Meadow, A. M., Wyborn, C., Klenk, N., Arnott, J. C., Ardoin, N. M., Fieseler, C.,  
708 Moss, R. H., Nichols, L., Stults, M., Vaughan, C., and Wong-Parodi, G.: Actionable knowledge and the art of  
709 engagement, *Current Opinion in Environmental Sustainability*, 42, 30–37,  
710 <https://doi.org/10.1016/j.cosust.2020.01.002>, 2020.

711 Mankin, J. S., Lehner, F., Coats, S., and McKinnon, K. A.: The Value of Initial Condition Large Ensembles to  
712 Robust Adaptation Decision-Making, *Earth's Future*, 8, <https://doi.org/10.1029/2020EF001610>, 2020.

713 McCrary, R. R., McGinnis, S., and Mearns, L. O.: Evaluation of Snow Water Equivalent in NARCCAP  
714 Simulations, Including Measures of Observational Uncertainty, *Journal of Hydrometeorology*, 18, 2425–2452,  
715 <https://doi.org/10.1175/JHM-D-16-0264.1>, 2017.

716 McCrary, R. R., Mearns, L. O., Hughes, M., Biner, S., and Bukovsky, M. S.: Projections of North American  
717 snow from NA-CORDEX and their uncertainties, with a focus on model resolution, *Climatic Change*, 170, 20,  
718 <https://doi.org/10.1007/s10584-021-03294-8>, 2022.

719 McMillan, H. K.: A review of hydrologic signatures and their applications, *WIREs Water*, 8, e1499,  
720 <https://doi.org/10.1002/wat2.1499>, 2021.

721 Meehl, G. A., Goddard, L., Murphy, J., Stouffer, R. J., Boer, G., Danabasoglu, G., Dixon, K., Giorgetta, M. A.,  
722 Greene, A. M., Hawkins, E., Hegerl, G., Karoly, D., Keenlyside, N., Kimoto, M., Kirtman, B., Navarra, A.,  
723 Pulwarty, R., Smith, D., Stammer, D., and Stockdale, T.: Decadal Prediction, *Bulletin of the American*  
724 *Meteorological Society*, 90, 1467–1485, <https://doi.org/10.1175/2009BAMS2778.1>, 2009.

725 Mizukami, N., Rakovec, O., Newman, A. J., Clark, M. P., Wood, A. W., Gupta, H. V., and Kumar, R.: On the  
726 choice of calibration metrics for “high-flow” estimation using hydrologic models, *Hydrol. Earth Syst. Sci.*, 23,  
727 2601–2614, <https://doi.org/10.5194/hess-23-2601-2019>, 2019.

728 Moise, A., Wilson, L., Grose, M., Whetton, P., Watterson, I., Bhend, J., Bathols, J., Hanson, L., Erwin, T.,  
729 Bedin, T., Heady, C., and Rafter, T.: Evaluation of CMIP3 and CMIP5 models over the Australian region to  
730 inform confidence in projections, *AMOJ*, 65, 19–53, <https://doi.org/10.22499/2.6501.004>, 2015.

731 Mukherjee, S., Mishra, A., and Trenberth, K. E.: Climate Change and Drought: a Perspective on Drought  
732 Indices, *Curr Clim Change Rep*, 4, 145–163, <https://doi.org/10.1007/s40641-018-0098-x>, 2018.

733 Newman, A. J., Clark, M. P., Craig, J., Nijssen, B., Wood, A., Gutmann, E., Mizukami, N., Brekke, L., and  
734 Arnold, J. R.: Gridded Ensemble Precipitation and Temperature Estimates for the Contiguous United States,  
735 *Journal of Hydrometeorology*, 16, 2481–2500, <https://doi.org/10.1175/JHM-D-15-0026.1>, 2015.

736 O'Neill, B. C., Kriegler, E., Ebi, K. L., Kemp-Benedict, E., Riahi, K., Rothman, D. S., van Ruijven, B. J., van  
737 Vuuren, D. P., Birkmann, J., Kok, K., Levy, M., and Solecki, W.: The roads ahead: Narratives for shared  
738 socioeconomic pathways describing world futures in the 21st century, *Global Environmental Change*, 42,  
739 169–180, <https://doi.org/10.1016/j.gloenvcha.2015.01.004>, 2017.

740 Pacchetti, M. B., Dessai, S., Bradley, S., and Stainforth, D. A.: Assessing the Quality of Regional Climate  
741 Information, *Bulletin of the American Meteorological Society*, 102, E476–E491,  
742 <https://doi.org/10.1175/BAMS-D-20-0008.1>, 2021.

743 Pardé, M.: *Fleuves et Rivières*, Collection Armand Collin. Section de Géographie (France), Fre No. 155, 1933.

744 Phillips, A., Deser, C., Fasullo, J., Schneider, D. P., and Simpson, I. R.: Assessing Climate Variability and  
745 Change in Model Large Ensembles: A User’s Guide to the “Climate Variability Diagnostics Package for Large  
746 Ensembles,” <https://doi.org/10.5065/H7C7-F961>, 2020.

747 Pierce, D. W., Su, L., Cayan, D. R., Risser, M. D., Livneh, B., and Lettenmaier, D. P.: An extreme-preserving  
748 long-term gridded daily precipitation data set for the conterminous United States, *Journal of Hydrometeorology*,  
749 <https://doi.org/10.1175/JHM-D-20-0212.1>, 2021.

750 Raff, D. A., Brekke, L. D., Werner, K. V., Wood, A. W., and White, K. D.: Short-Term Water Management  
751 Decisions: User Needs for Improved Climate, Weather, and Hydrologic Information, Bureau of Reclamation,  
752 U.S. Army Corps of Engineers and National Oceanic and Atmospheric Administration, 2013.

753 Reba, M. L., Marks, D., Seyfried, M., Winstral, A., Kumar, M., and Flerchinger, G.: A long-term data set for  
754 hydrologic modeling in a snow-dominated mountain catchment: A 25 YEAR DATA SET FOR HYDROLOGIC  
755 MODELING, *Water Resour. Res.*, 47, <https://doi.org/10.1029/2010WR010030>, 2011.

756 Reclamation: Technical Guidance for Incorporating Climate Change Information into Water Resources Planning  
757 Studies, U.S. Department of the Interior. Bureau of Reclamation, Denver, Colorado, 2014.

758 Reclamation: SECURE Water Act Section 9503(c) - Reclamation Climate Change and Water. Prepared for  
759 United States Congress., U.S. Department of the Interior. Bureau of Reclamation, Denver, Colorado, 2016.

760 Reed, K. A., Goldenson, N., Grotjahn, R., Gutowski, W. J., Jagannathan, K., Jones, A. D., Leung, L. R.,  
761 McGinnis, S. A., Pryor, S. C., Srivastava, A. K., Ullrich, P. A., and Zarzycki, C. M.: Metrics as tools for  
762 bridging climate science and applications, *Wiley Interdisciplinary Reviews: Climate Change*, 13, e799, 2022.

763 Regional Water Authority: Sacramento Regional Water Bank: A sustainable storage and recovery program,  
764 2019.

765 Riahi, K., van Vuuren, D. P., Kriegler, E., Edmonds, J., O’Neill, B. C., Fujimori, S., Bauer, N., Calvin, K.,  
766 Dellink, R., Fricko, O., Lutz, W., Popp, A., Cuaresma, J. C., KC, S., Leimbach, M., Jiang, L., Kram, T., Rao, S.,  
767 Emmerling, J., Ebi, K., Hasegawa, T., Havlik, P., Humpenöder, F., Da Silva, L. A., Smith, S., Stehfest, E.,  
768 Bosetti, V., Eom, J., Gernaat, D., Masui, T., Rogelj, J., Strefler, J., Drouet, L., Krey, V., Luderer, G., Harmsen,  
769 M., Takahashi, K., Baumstark, L., Doelman, J. C., Kainuma, M., Klimont, Z., Marangoni, G., Lotze-Campen,  
770 H., Obersteiner, M., Tabeau, A., and Tavoni, M.: The Shared Socioeconomic Pathways and their energy, land  
771 use, and greenhouse gas emissions implications: An overview, *Global Environmental Change*, 42, 153–168,  
772 <https://doi.org/10.1016/j.gloenvcha.2016.05.009>, 2017.

773 Rodgers, K. B., Lee, S.-S., Rosenbloom, N., Timmermann, A., Danabasoglu, G., Deser, C., Edwards, J., Kim,  
774 J.-E., Simpson, I. R., Stein, K., Stuecker, M. F., Yamaguchi, R., Bódai, T., Chung, E.-S., Huang, L., Kim, W. M.,  
775 Lamarque, J.-F., Lombardozzi, D. L., Wieder, W. R., and Yeager, S. G.: Ubiquity of human-induced changes in  
776 climate variability, *Earth Syst. Dynam.*, 12, 1393–1411, <https://doi.org/10.5194/esd-12-1393-2021>, 2021.

777 Rugg, A., Gutmann, E. D., McCrary, R. R., Lehner, F., Newman, A. J., Richter, J. H., Tye, M. R., and Wood, A.  
778 W.: Mass-Conserving Downscaling of Climate Model Precipitation over Mountainous Terrain for Water  
779 Resource Applications, *Geophysical Research Letters*, 50, 20, e2023GL105326.  
780 <http://dx.doi.org/10.1029/2023GL105326>, 2023.

781 Seaber, P. R., Kapiros, F. P., and Knapp, G. L.: Hydrologic Unit Maps, U.S. Geological Survey, 1987.

782 Sedláček, J. and Knutti, R.: Half of the world's population experience robust changes in the water cycle for a 2  
783 °C warmer world, *Environ. Res. Lett.*, 9, 044008, <https://doi.org/10.1088/1748-9326/9/4/044008>, 2014.

784 Shepherd, T. G., Boyd, E., Calel, R. A., Chapman, S. C., Dima-West, I. M., Fowler, H. J., James, R., Maraun,  
785 D., Martius, O., Senior, C. A., Sobel, A. H., Stainforth, D. A., Tett, B., Trenberth, K. E., Hurk, B. J., Watkin, N.  
786 W., Wilby, R. L., and Zenghelis, D. A.: Storylines: An alternative approach to representing uncertainty in  
787 physical aspects of climate change, *Climatic Change*, 151, 555–571,  
788 <https://doi.org/10.1007/s10584-018-2317-9>, 2018.

789 Simpson, I. R., Lawrence, D. M., Swenson, S. C., Hannay, C., McKinnon, K. A., and Truesdale, J. E.:  
790 Improvements in Wintertime Surface Temperature Variability in the Community Earth System Model Version 2  
791 (CESM2) Related to the Representation of Snow Density, *J Adv Model Earth Syst*, 14,  
792 <https://doi.org/10.1029/2021MS002880>, 2022.

793 Tebaldi, C. and Knutti, R.: The use of the multi-model ensemble in probabilistic climate projections,  
794 *Philosophical Transactions of the Royal Society A: Mathematical, Physical and Engineering Sciences*, 365,  
795 2053–2075, <https://doi.org/10.1098/rsta.2007.2076>, 2007.

796 Tebaldi, C., Dorheim, K., Wehner, M., and Leung, R.: Extreme metrics from large ensembles: investigating the  
797 effects of ensemble size on their estimates, *Earth Syst. Dynam.*, 12, 1427–1501,  
798 <https://doi.org/10.5194/esd-12-1427-2021>, 2021.

799 Tye, M.: Water Availability Metrics August 2021 Workshop Report, Open Science Framework,  
800 <https://doi.org/10.17605/OSF.IO/M7NXD>, 2023.

801 Tye, M. R., Holland, G. J., and Done, J. M.: Rethinking failure: time for closer engineer–scientist collaborations  
802 on design, *Proceedings of the Institution of Civil Engineers - Forensic Engineering*, 168, 49–57,  
803 <https://doi.org/10.1680/feng.14.00004>, 2015.

804 Underwood, E. C., Hollander, A. D., Flint, L. E., Flint, A. L., and Safford, H. D.: Climate change impacts on  
805 hydrological services in southern California, *Environ. Res. Lett.*, 13, 124019,  
806 <https://doi.org/10.1088/1748-9326/aacb59>, 2018.

807 Vano, J. A., Udall, B., Cayan, D. R., Overpeck, J. T., Brekke, L. D., Das, T., Hartmann, H. C., Hidalgo, H. G.,  
808 Hoerling, M., McCabe, G. J., Morino, K., Webb, R. S., Werner, K., and Lettenmaier, D. P.: Understanding  
809 Uncertainties in Future Colorado River Streamflow, *Bulletin of the American Meteorological Society*, 95,  
810 59–78, <https://doi.org/10.1175/BAMS-D-12-00228.1>, 2014.

811 Wagener, T., Reinecke, R., and Pianosi, F.: On the evaluation of climate change impact models, *WIREs Climate  
812 Change*, 13, e772, <https://doi.org/10.1002/wcc.772>, 2022.

813 Wood, R. R., Lehner, F., Pendergrass, A. G., and Schlunegger, S.: Changes in precipitation variability across  
814 time scales in multiple global climate model large ensembles, *Environ. Res. Lett.*, 16, 084022,  
815 <https://doi.org/10.1088/1748-9326/ac10dd>, 2021.

816 Wright, D. B., Bosma, C. D., and Lopez-Cantu, T.: U.S. Hydrologic Design Standards Insufficient Due to Large  
817 Increases in Frequency of Rainfall Extremes, *Geophys. Res. Lett.*, 46, 8144–8153,  
818 <https://doi.org/10.1029/2019GL083235>, 2019.

819 Yuan, H., Toth, Z., Peña, M., and Kalnay, E.: Overview of Weather and Climate Systems, in: Handbook of  
820 Hydrometeorological Ensemble Forecasting, edited by: Duan, Q., Pappenberger, F., Wood, A., Cloke, H. L., and  
821 Schaake, J. C., Springer, Berlin, Heidelberg, 35–65, [https://doi.org/10.1007/978-3-642-39925-1\\_10](https://doi.org/10.1007/978-3-642-39925-1_10), 2019.  
822 Zhang, X., Alexander, L., Hegerl, G. C., Jones, P., Tank, A. K., Peterson, T. C., Trewin, B., and Zwiers, F. W.:  
823 Indices for monitoring changes in extremes based on daily temperature and precipitation data, Wiley  
824 Interdisciplinary Reviews: Climate Change, 2, 851–870, <https://doi.org/10.1002/wcc.147>, 2011.  
825  
826